



Search for high-mass new phenomena in the dilepton final state using proton–proton collisions at $\sqrt{s} = 13$ TeV with the ATLAS detector



The ATLAS Collaboration ^{*}

ARTICLE INFO

Article history:

Received 14 July 2016

Received in revised form 17 August 2016

Accepted 24 August 2016

Available online 30 August 2016

Editor: W.-D. Schlatter

ABSTRACT

A search is conducted for both resonant and non-resonant high-mass new phenomena in dielectron and dimuon final states. The search uses 3.2 fb^{-1} of proton–proton collision data, collected at $\sqrt{s} = 13$ TeV by the ATLAS experiment at the LHC in 2015. The dilepton invariant mass is used as the discriminating variable. No significant deviation from the Standard Model prediction is observed; therefore limits are set on the signal model parameters of interest at 95% credibility level. Upper limits are set on the cross-section times branching ratio for resonances decaying to dileptons, and the limits are converted into lower limits on the resonance mass, ranging between 2.74 TeV and 3.36 TeV, depending on the model. Lower limits on the $\ell\ell qq$ contact interaction scale are set between 16.7 TeV and 25.2 TeV, also depending on the model.

© 2016 The Author. Published by Elsevier B.V. This is an open access article under the CC BY license (<http://creativecommons.org/licenses/by/4.0/>). Funded by SCOAP³.

1. Introduction

The dilepton (ee or $\mu\mu$) final-state signature has excellent sensitivity to a wide variety of new phenomena expected in theories beyond the Standard Model (SM). It benefits from high signal selection efficiencies and relatively small, well-understood backgrounds.

Models with extended gauge groups often feature additional $U(1)$ symmetries with corresponding heavy spin-1 Z' bosons whose decays would manifest themselves as narrow resonances in the dilepton mass spectrum. Grand Unified Theories (GUT) have inspired models based on the E_6 gauge group [1,2], which, for a particular choice of symmetry-breaking pattern, includes two neutral gauge bosons that mix with an angle θ_{E_6} . This yields a physical state defined by $Z'(\theta_{E_6}) = Z'_\psi \cos \theta_{E_6} + Z'_\chi \sin \theta_{E_6}$, where the gauge fields Z'_ψ and Z'_χ are associated with two separate $U(1)$ groups resulting from the breaking of the E_6 symmetry. All Z' signals in this model are defined by specific values of θ_{E_6} ranging from $-\pi$ to π , and the six commonly motivated cases are investigated in this search, namely Z'_ψ , Z'_η , Z'_N , Z'_1 , Z'_S , and Z'_χ . The widths of these states vary from 0.5% to 1.2% of the resonance mass, respectively. In addition to the GUT-inspired E_6 models, the Sequential Standard Model (SSM) [2] provides a common benchmark model that includes a Z'_{SSM} boson with couplings to fermions identical to those of the SM Z boson. This search is also sensitive to a series of models that predict the presence of narrow dilepton res-

onances; however constraints are not explicitly evaluated on these models. These include the Randall–Sundrum (RS) model [3] with a warped extra dimension giving rise to spin-2 graviton excitations, the quantum black hole model [4], the Z^* model [5], and the minimal walking technicolour model [6].

Some models of physics beyond the SM result in non-resonant deviations from the predicted SM dilepton mass spectrum. Compositeness models motivated by the repeated pattern of quark and lepton generations predict new interactions involving their constituents. These interactions may be represented as a contact interaction (CI) between initial-state quarks and final-state leptons [7, 8]. Other models producing non-resonant effects, but not explicitly evaluated here, are models with large extra dimensions [9] motivated by the hierarchy problem. The following four-fermion CI Lagrangian [7,8] is used to describe a new interaction or compositeness in the process $q\bar{q} \rightarrow \ell^+\ell^-$:

$$\mathcal{L} = \frac{g^2}{\Lambda^2} [\eta_{\text{LL}} (\bar{q}_L \gamma_\mu q_L) (\bar{\ell}_L \gamma^\mu \ell_L) + \eta_{\text{RR}} (\bar{q}_R \gamma_\mu q_R) (\bar{\ell}_R \gamma^\mu \ell_R) + \eta_{\text{LR}} (\bar{q}_L \gamma_\mu q_L) (\bar{\ell}_R \gamma^\mu \ell_R) + \eta_{\text{RL}} (\bar{q}_R \gamma_\mu q_R) (\bar{\ell}_L \gamma^\mu \ell_L)], \quad (1)$$

where g is a coupling constant set to be $\sqrt{4\pi}$ by convention, Λ is the CI scale, and $q_{L,R}$ and $\ell_{L,R}$ are left-handed and right-handed quark and lepton fields, respectively. The symbol γ_μ denotes the gamma matrices, and the parameters η_{ij} , where i and j are L or R (left or right), define the chiral structure of the new interaction. Different chiral structures are investigated here, with the left–right (right–left) model obtained by setting $\eta_{\text{LR}} = \pm 1$ ($\eta_{\text{RL}} = \pm 1$) and all other parameters to zero. Likewise, the left–left and right–right models are obtained by setting the corresponding parameters to

^{*} E-mail address: atlas.publications@cern.ch.

± 1 , and the others to zero. The sign of η_{ij} determines whether the interference between the SM Drell–Yan (DY) $q\bar{q} \rightarrow Z/\gamma^* \rightarrow \ell^+\ell^-$ process and the CI process is constructive ($\eta_{ij} = -1$) or destructive ($\eta_{ij} = +1$).

The most sensitive previous searches for a Z' decaying to the dilepton final state were carried out by the ATLAS and CMS Collaborations [10,11]. Using 20 fb^{-1} of pp collision data at $\sqrt{s} = 8 \text{ TeV}$, ATLAS set a lower limit at 95% credibility level (CL) on the Z'_{SSM} pole mass of 2.90 TeV for the combined ee and $\mu\mu$ channels. Similar limits were set by CMS. The most stringent constraints on CI searches are also provided by the CMS and ATLAS Collaborations [11,12]. The strongest lower limits on the $\ell\ell qq$ CI scale are $\Lambda > 21.6 \text{ TeV}$ and $\Lambda > 17.2 \text{ TeV}$ at 95% CL for constructive and destructive interference, respectively, in the case of left–left interactions and given a uniform positive prior in $1/\Lambda^2$. Previous dilepton searches at ATLAS have also set lower limits on the resonance mass in other models such as: an RS graviton up to 2.68 TeV, quantum black holes at 3.65 TeV, the Z^* boson at 2.85 TeV, and minimal walking technicolour up to 2.27 TeV [10]. Similar lower limits were set by CMS where equivalent searches were performed [11].

In this letter, a search for resonant and non-resonant new phenomena is presented using the observed ee and $\mu\mu$ mass spectra extracted from pp collisions within the ATLAS detector at the Large Hadron Collider (LHC) operating at $\sqrt{s} = 13 \text{ TeV}$. The pp collision data correspond to an integrated luminosity of 3.2 fb^{-1} . The analysis and interpretation of these spectra rely primarily on simulated samples of signal and background processes. The Z mass peak region is used to normalise the background contribution and perform cross-checks of the simulated samples. The interpretation is then performed taking into account the expected shape of different signals in the dilepton mass distribution.

2. ATLAS detector

The ATLAS experiment [13,14] at the LHC is a multi-purpose particle detector with a forward–backward symmetric cylindrical geometry and near 4π coverage in solid angle.¹ It consists of an inner tracking detector surrounded by a thin superconducting solenoid providing a 2 T axial magnetic field, electromagnetic and hadronic calorimeters, and a muon spectrometer. The inner tracking detector (ID) covers the pseudorapidity range $|\eta| < 2.5$. It consists of silicon pixel, silicon microstrip, and transition–radiation tracking detectors. Lead/liquid-argon (LAr) sampling calorimeters provide electromagnetic (EM) energy measurements with high granularity. A hadronic (steel/scintillator-tile) calorimeter covers the central pseudorapidity range ($|\eta| < 1.7$). The endcap and forward regions are instrumented with LAr calorimeters for EM and hadronic energy measurements up to $|\eta| = 4.9$. The total thickness of the EM calorimeter is more than twenty radiation lengths. The muon spectrometer (MS) surrounds the calorimeters and is based on three large superconducting air-core toroids with eight coils each. The field integral of the toroids ranges between 2.0 and $6.0 \text{ T} \cdot \text{m}$ for most of the detector. It includes a system of precision tracking chambers and fast detectors for triggering. A dedicated trigger system is used to select events. The first-level trigger is implemented in hardware and uses the calorimeter and muon detectors to reduce the accepted event rate from 40 MHz to below

100 kHz. This is followed by a software-based trigger that reduces the accepted event rate to 1 kHz on average.

3. Data and Monte Carlo samples

The data sample used in this analysis was collected during the 2015 LHC run with pp collisions at $\sqrt{s} = 13 \text{ TeV}$. After selecting periods with stable beams and requiring that relevant detector systems are functional, the data set used for the analysis corresponds to 3.2 fb^{-1} of integrated luminosity. Event quality is also checked to remove those events which contain noise bursts or coherent noise in the calorimeters.

Modelling of the various background sources relies primarily on Monte Carlo (MC) simulation. The dominant background contribution arises from the DY process [15]. Other background sources are top-quark [16] and diboson (WW , WZ , ZZ) [17] production. In the case of the dielectron channel, multi-jet and W + jets processes also contribute due to the misidentification of jets as electrons. A data-driven method, described in Section 5, is used to estimate these background contributions. The multi-jet and W + jets contribution in the dimuon channel is negligible.

DY events are simulated using POWHEG-BOX v2 [18] at next-to-leading order (NLO) in Quantum Chromodynamics (QCD), and interfaced to the PYTHIA 8.186 [19] parton shower model. The CT10 parton distribution function (PDF) set [20] is used in the matrix element calculation. The AZNLO [21] set of tuned parameters (“tune”) is used, with the CTEQ6L1 PDF set [22], for the modelling of non-perturbative effects. The EvtGen v1.2.0 program [23] is used for properties of the bottom and charm hadron decays. PHOTOS++ version 3.52 [24] is used for Quantum Electrodynamics (QED) emissions from electroweak vertices and charged leptons. Event yields are corrected with a mass-dependent rescaling to next-to-next-to-leading order (NNLO) in the QCD coupling constant, computed with VRAP 0.9 [25] and the CT14NNLO PDF set [26]. The NNLO QCD corrections are a factor of ~ 0.98 at $m_{\ell\ell} = 3 \text{ TeV}$. Mass-dependent electroweak (EW) corrections are computed at NLO with MCSANC 1.20 [27]. The NLO EW corrections are a factor of ~ 0.86 at $m_{\ell\ell} = 3 \text{ TeV}$. Those include photon-induced contributions ($\gamma\gamma \rightarrow \ell\ell$ via t - and u -channel processes) computed with the MRST2004QED PDF set [28].

Diboson processes with four charged leptons, three charged leptons and one neutrino, or two charged leptons and two neutrinos are simulated using the SHERPA 2.1.1 generator [29]. Matrix elements contain all diagrams with four electroweak vertices. They are calculated for up to one (4ℓ , $2\ell + 2\nu$) or no additional partons ($3\ell + 1\nu$) at NLO. Diboson processes with one of the bosons decaying hadronically and the other leptonically are simulated using the SHERPA 2.1.1 generator. They are calculated for up to one (ZZ) or no (WW , WZ) additional partons at NLO. All are calculated with up to three additional partons at leading-order (LO) using the Comix [30] and OpenLoops [31] matrix element generators and merged with the SHERPA parton shower [32] using the ME+PS@NLO prescription [33]. The CT10 PDF set is used in conjunction with dedicated parton shower tuning developed by the SHERPA authors. The SHERPA diboson sample cross-section was scaled down to account for its use of $\alpha_{\text{QED}} = 1/129$ rather than $1/132$ corresponding to the use of current PDG parameters as input to the G_μ scheme.

For the generation of $t\bar{t}$ and single top quarks in the Wt -channel and s -channel the POWHEG-BOX v2 generator with the CT10 PDF set in the matrix element calculations is used. EW t -channel single-top-quark events are generated using the POWHEG-BOX v1 generator. This generator uses the four-flavour scheme for the NLO matrix element calculations together with the fixed four-flavour PDF set CT10f4. For all top-quark processes, top-quark spin

¹ ATLAS Collaboration uses a right-handed coordinate system with its origin at the nominal interaction point (IP) in the centre of the detector and the z -axis along the beam pipe. The x -axis points from the IP to the centre of the LHC ring, and the y -axis points upwards. Cylindrical coordinates (r, ϕ) are used in the transverse plane, ϕ being the azimuthal angle around the z -axis. The pseudorapidity is defined in terms of the polar angle θ as $\eta = -\ln \tan(\theta/2)$. Angular distance is measured in units of $\Delta R \equiv \sqrt{(\Delta\eta)^2 + (\Delta\phi)^2}$.

correlations are preserved (for t -channel, top quarks are decayed using MadSpin [34]). The parton shower, fragmentation, and the underlying event are simulated using PYTHIA 6.428 [35] with the CTEQ6L1 PDF set and the Perugia 2012 tune (P2012) [36]. The top-quark mass is set to 172.5 GeV. The EvtGen v1.2.0 program is used for properties of the bottom and charm hadron decays. The $t\bar{t}$ and single-top-quark MC samples are normalised to a cross-section as calculated with the Top++ 2.0 program [37], which is accurate to NNLO in perturbative QCD, including resummation of next-to-next-to-leading logarithmic soft gluon terms.

Resonant and non-resonant signal processes are produced at LO using PYTHIA 8.186 with the NNPDF23LO PDF set [38] and A14 tune [39] for event generation, parton showering and hadronisation. In the case of Z' production, interference effects (such as with DY production) are not included. However, for the production of non-resonant signal events, both the DY and CI events are generated together in the same sample to account for the significant interference effects between those two processes. Higher-order QCD corrections are computed as for the DY background and applied to both the resonant and non-resonant MC samples. EW corrections are not applied to the resonant MC samples due to the large model dependence. However, these corrections are applied to the non-resonant MC samples as they involve interference between the DY and CI processes. Moreover, including the EW corrections leads to a more conservative estimate when setting exclusion limits. The generator settings and corrections described here are also used to compute the signal cross-sections and branching ratios.

The detector response is simulated with GEANT 4 [40,41] and the events are processed with the same reconstruction software as used for the data. Furthermore, the distribution of the number of additional simulated pp collisions in the same or neighbouring beam crossings (pile-up) is accounted for by overlaying simulated minimum-bias events and re-weighting the MC to match the distribution observed in the data.

4. Event selection

Electrons are reconstructed in the central region of the ATLAS detector covered by the tracking detectors ($|\eta| < 2.47$), by combining calorimetric and tracking information as described in Ref. [42]. The transition region between the central and forward regions of the calorimeters, in the range $1.37 \leq |\eta| \leq 1.52$, exhibits degraded energy resolution and is therefore excluded. A likelihood discriminant is built to suppress electron candidates resulting from hadronic jets, photon conversions, Dalitz decays and semileptonic heavy-flavour hadron decays. The likelihood discriminant utilises lateral and longitudinal shower shape, tracking and cluster-track matching quantities. Several operating points are defined for the likelihood discrimination, as described in Ref. [42]. In this analysis, the *Medium* working point is used in the search, and the *Very Loose* and *Loose* working points are used in the data-driven background estimation described in Section 5. In addition to the likelihood discriminant, selection criteria based on track quality are applied. The selection efficiency smoothly decreases from 96% to 95% for electrons with transverse energy (E_T) between 500 GeV and 1.5 TeV. The selection efficiency modelling is evaluated in the data using a tag-and-probe method [43] up to E_T of 500 GeV and the uncertainties due to the modelling of the shower shape variables are evaluated as described in Section 6. The electron energy scale and resolution has been calibrated up to E_T of 500 GeV using data taken at $\sqrt{s} = 8$ TeV [44]. The energy resolution for high- E_T electrons is approximately 1%. To suppress background from misidentified jets as well as from light- and heavy-flavour hadron decays inside jets, electrons are required to satisfy the calorimeter-based and track-based isolation criteria with a fixed efficiency of 99%

over the full range of electron momentum. The calorimeter-based isolation relies on the ratio of the total energy deposited in a cone of size $\Delta R = 0.2$ centred at the electron cluster barycentre to the electron E_T . Likewise, the track-based isolation relies on the ratio of the scalar sum of transverse momenta of tracks within a cone of size $\Delta R = 10$ GeV/ p_T to the transverse momentum (p_T) of the electron track. The tracks are required to originate from the primary vertex (defined as the vertex with the highest sum of track p_T^2), have $p_T > 1$ GeV, $|\eta| < 2.5$, and meet track quality criteria.

Candidate muon tracks are, at first, reconstructed independently in the ID and the MS [45]. The two tracks are then used as input to a combined fit which takes into account the energy loss in the calorimeter and multiple-scattering effects. The ID track used for the combined fit is required to be within the ID acceptance, $|\eta| < 2.5$, and to have a minimum number of hits in each ID sub-system. Muon candidates in the overlap of the MS barrel and endcap region ($1.01 < |\eta| < 1.10$) are rejected due to the potential for p_T mismeasurement resulting from relative barrel-endcap misalignment. In order to reduce the background from light- and heavy-hadron decays inside jets, muons are required to fulfil relative track-based isolation requirements with a fixed efficiency of 99%, as defined above for electron candidates. The selected muon candidates must also pass near the primary interaction point in the z coordinate to suppress cosmic-ray background. Since momentum resolution is a key ingredient of this analysis, muon tracks are required to have at least three hits in each of three precision chambers in the MS and not to traverse regions of the MS which are poorly aligned. This requirement reduces the muon reconstruction efficiency by about 20% for muons with a p_T greater than 1.5 TeV. Finally, the q/p (charge divided by momentum) measurements performed independently in the ID and MS must agree within seven standard deviations, calculated from the sum in quadrature of the ID and MS momentum uncertainties.

To search for high-mass dilepton signatures of new physics, requirements are applied to the data and MC samples to select events with two high- E_T electrons or high- p_T muons, satisfying the criteria described above. In the dielectron channel, a two-electron trigger based on the *Loose* identification criteria with an E_T threshold of 17 GeV for each electron is used. Events in the dimuon channel are required to pass at least one of two single-muon triggers with p_T thresholds of 26 GeV and 50 GeV, with the former also requiring the muon to be isolated. These triggers select events from a simulated sample of Z'_χ with a pole mass of 3 TeV with an efficiency of about 87% and 94% for the dielectron and dimuon channels, respectively. Electron (muon) candidates are required to have E_T (p_T) greater than 30 GeV and have a transverse impact parameter consistent with the beam-line. Events are required to have at least one reconstructed primary vertex and at least one pair of same-flavour lepton candidates.

Only the electron (muon) pair with the highest scalar sum of E_T (p_T) is retained in each event and an opposite-charge requirement is applied in the dimuon case. The opposite-charge requirement is not applied in the dielectron channel due to higher chance of charge misidentification for high- E_T electrons.

Energy (momentum) calibration and resolution smearing are applied to electron (muon) candidates in the simulated samples to match the performance observed in data [44,45]. Event-level corrections are applied in the simulated samples to match the trigger, reconstruction and isolation efficiencies.

Representative values of the total acceptance times efficiency for a Z'_χ boson with a pole mass of 3 TeV are 69% in the dielectron channel and 46% in the dimuon channel.

5. Background estimation

The backgrounds from processes producing two real leptons in the final state are modelled using MC simulated samples as described in Section 3. The processes for which MC simulation is used are: DY, $t\bar{t}$ and single-top-quark, and diboson (WW , WZ , and ZZ) production. The simulated samples for the top-quark (single and pair) production and diboson production are not large enough to model the dilepton mass distribution above several hundred GeV. Therefore, fits to the dilepton invariant mass spectrum ($m_{\ell\ell}$) using monotonically decreasing functions are used to extrapolate these background processes to dilepton masses above 600 GeV.

In the dimuon channel, contributions from W + jets and multi-jet production are negligible, and therefore are not included in the expected yield. However, the W + jets, multi-jet and other production processes, where at most one real electron is produced, do contribute to the selected ee sample due to their having one or more hadronic jets satisfying the electron selection criteria. The contribution from these processes is estimated simultaneously with a data-driven technique, the *matrix method*, described in Ref. [10]. In this technique, probabilities for electrons and jets to pass electron candidate selection are used. Probabilities of electron identification are estimated from MC simulated DY samples in several bins of E_T and $|\eta|$. Probabilities of jet misidentification as an electron in different E_T bins are estimated in data samples triggered on the presence of a *Very Loose* or a *Loose* electron candidate. The estimate is extrapolated by fitting a smooth function to the m_{ee} distribution between 150 and 600 GeV to mitigate effects of limited event counts in the high-mass region and method instability in the Z peak region. The uncertainties in this background estimate are evaluated by considering differences in the estimates for events with same-charge and opposite-charge electrons as well as by varying the electron identification probabilities and changing the parameters of the extrapolation functions.

As a final step, the sums of backgrounds estimated using MC samples are rescaled independently in both channels so that the estimated count of events matches the data in the Z -peak normalisation region $80 \text{ GeV} < m_{\ell\ell} < 120 \text{ GeV}$. This normalisation procedure is found to agree with the equivalent scaling using the expected integrated luminosity within 2% for both channels (and in the same direction), which is well within the current luminosity uncertainty of 5%. The luminosity uncertainty was calculated using the same methodology as for the 7 TeV data [46].

6. Systematic uncertainties

As a result of the background yield normalisation described above, the background prediction is insensitive to the luminosity uncertainty as well as any other mass-independent effect. Signal scaling is performed using the event counts in the data in the Z -peak region. Therefore, a uniform uncertainty of 4% due to the uncertainty in the Z/γ^* cross-section in the normalisation region is applied to signal. This uncertainty was obtained using a calculation based on VRAP at NNLO evaluating the effect of varying the PDF sets, scales and α_S . Mass-dependent systematic uncertainties, on the other hand, are considered as nuisance parameters in the statistical interpretation and include both the theoretical and experimental effects on the total background and experimental effects on the signal. Systematic uncertainties common to the dielectron and dimuon channels are treated as correlated where relevant. All systematic uncertainties estimated to have an impact $< 3\%$ on the total expected number of events for all values of $m_{\ell\ell}$ are neglected, as they have a negligible impact on the results of the search.

Theoretical uncertainties in the background prediction are dominated by the DY background in this search. They arise from the PDF eigenvector variations of the nominal PDF set, as well as variations of PDF scale, α_S , EW corrections, and photon-induced (PI) corrections. The effects of different PDF set choices are also considered. The theoretical uncertainties are the same at generator level for the dielectron and dimuon channels, but result in different uncertainties at reconstruction level, due to the differing resolutions between the two channels. The PDF variation uncertainty is obtained using the 90% C.L. CT14NNLO PDF error set and by following the procedure described in Refs. [10,47,48]. Rather than using a single nuisance parameter to describe the 28 eigenvectors of this PDF error set, which could lead to an underestimation of its effect, a re-diagonalised set of 7 PDF eigenvectors was used [26], which are treated as separate nuisance parameters. The sum in quadrature of these eigenvectors matches the original CT14NNLO error envelope well. The uncertainties due to the variation of PDF scale and α_S are derived using VRAP with the former obtained by varying the renormalisation and factorisation scales of the nominal CT14NNLO PDF up and down simultaneously by a factor of two. The value of α_S used (0.118) is varied by ± 0.003 . The EW correction uncertainty was assessed by comparing the nominal additive $(1 + \delta_{EW} + \delta_{QCD})$ treatment with the multiplicative approximation $((1 + \delta_{EW})(1 + \delta_{QCD}))$ treatment of the EW correction in the combination of the higher-order EW and QCD effects. The uncertainty in the photon-induced correction is calculated based on the uncertainty of the quark masses and the photon PDF. An additional uncertainty is derived due to the choice of nominal PDF set, by comparing the central values of CT14NNLO with those from other PDF sets as recommended by the PDF4LHC forum [48], namely MMHT14 [49] and NNPDF3.0 [50]. The maximum absolute deviation from the envelope of these comparisons is used as the PDF choice uncertainty, where it is larger than the CT14NNLO PDF eigenvector variation envelope. Theoretical uncertainties are not applied to the signal prediction in the statistical interpretation.

Theoretical uncertainties in the $t\bar{t}$ and diboson backgrounds were also considered. The $t\bar{t}$ MC sample is normalised to a cross-section of $\sigma_{t\bar{t}} = 832_{-29}^{+20}$ (scale) ± 35 (PDF + α_S) pb, calculated with the Top++ 2.0 program as described in Section 3. The first uncertainty comes from the independent variation of the factorisation and renormalisation scales, μ_F and μ_R , while the second one is associated to variations in the PDF and α_S , following the PDF4LHC prescription [48]. Normalisation uncertainties in the top quarks and diboson background were found to be negligible. The uncertainties in the top-quark and diboson background extrapolations are estimated by varying both the functional form and the fit range, taking the envelope of all variations. These uncertainties were also found to be negligible with respect to the total background estimate. Both sources of systematic uncertainty in these background contributions are included in the “Top quarks & dibosons” entry in Table 1.

The following sources of experimental uncertainty are accounted for: lepton trigger, identification, reconstruction, and isolation efficiency, lepton energy scale and resolution, multi-jet and W + jets background estimate, and MC statistics. Efficiencies are evaluated using events from the $Z \rightarrow \ell\ell$ peak and then extrapolated to high energies. The uncertainty in the muon reconstruction efficiency is the largest experimental uncertainty in the dimuon channel. It includes the uncertainty obtained from $Z \rightarrow \mu\mu$ data studies and a high- p_T extrapolation uncertainty corresponding to the magnitude of the decrease in the muon reconstruction and selection efficiency with increasing p_T that is predicted by the MC simulation. The effect on the muon reconstruction efficiency was found to be approximately 3% per TeV as a function of muon p_T .

Table 1

Summary of the relative systematic uncertainties in the expected number of events at a dilepton mass of 2 TeV (3 TeV). The background estimate is normalised to data in the dilepton invariant mass window 80–120 GeV, and the values quoted for the uncertainty represent the relative change in the total expected number of events in the given $m_{\ell\ell}$ histogram bin containing the reconstructed $m_{\ell\ell}$ mass of 2 TeV (3 TeV). For the signal uncertainties the values were computed using a $Z'\chi$ signal model with a pole mass of 2 TeV (3 TeV) by comparing yields in the core of the mass peak (within the full width at half maximum) between the distribution varied by a given uncertainty and the nominal distribution. The total uncertainty quoted on the last line is obtained from a sum in quadrature of the individual uncertainties. “N/A” represents cases where the uncertainty is not applicable, and “negligible” represents cases where the uncertainty is smaller than 3% across the entire mass spectrum, which are neglected in the statistical interpretation.

Source	Dielectron		Dimuon	
	Signal	Background	Signal	Background
Normalisation	4.0% (4.0%)	N/A	4.0% (4.0%)	N/A
PDF choice	N/A	<1.0% (<1.0%)	N/A	<1.0% (<1.0%)
PDF variation	N/A	9.1% (13.5%)	N/A	8.2% (11.1%)
PDF scale	N/A	1.8% (2.3%)	N/A	1.7% (2.0%)
α_s	N/A	negligible	N/A	negligible
EW corrections	N/A	2.3% (3.9%)	N/A	2.0% (3.1%)
Photon-induced corrections	N/A	3.4% (5.4%)	N/A	3.1% (4.3%)
Top quarks & dibosons	N/A	negligible	N/A	negligible
Efficiency	5.4% (5.4%)	5.4% (5.4%)	13.6% (17.6%)	13.6% (17.6%)
Lepton scale & resolution	<1.0% (<1.0%)	3.7% (5.4%)	4.7% (4.8%)	2.3% (6.9%)
Multi-jet & W + jets	N/A	negligible	N/A	N/A
MC statistical	negligible	negligible	negligible	negligible
Total	6.7% (6.7%)	12.1% (17.0%)	14.9% (18.7%)	16.6% (22.6%)

Table 2

Expected and observed event yields in the dielectron (top) and dimuon (bottom) channels in different dilepton mass intervals. The quoted errors for the dominant Drell–Yan background correspond to the combined statistical, theoretical, and experimental systematic uncertainties. The errors quoted for the other background sources correspond to the combined statistical and experimental systematic uncertainties.

m_{ee} [GeV]	120–300	300–500	500–700	700–900	900–1200	1200–1800	1800–3000	3000–6000
Drell–Yan (Z/γ^*)	21000 ± 400	940 ± 50	149 ± 10	38.3 ± 3.0	16.5 ± 1.4	5.6 ± 0.6	0.78 ± 0.10	0.030 ± 0.005
Top quarks	4550 ± 110	446 ± 25	47.2 ± 1.6	6.2 ± 0.8	1.13 ± 0.35	0.12 ± 0.09	0.002 ± 0.006	< 0.001
Diboson	620 ± 10	67.5 ± 1.2	10.3 ± 0.9	2.3 ± 0.5	0.78 ± 0.28	0.20 ± 0.11	0.021 ± 0.018	< 0.001
Multi-jet & W + jets	320 ± 80	40 ± 12	7.2 ± 1.8	1.6 ± 0.8	0.5 ± 0.4	0.08 ± 0.10	0.002 ± 0.005	< 0.001
Total SM	26500 ± 400	1490 ± 60	214 ± 11	48.4 ± 3.2	18.9 ± 1.6	6.0 ± 0.6	0.81 ± 0.10	0.030 ± 0.006
Data	25951	1447	202	44	17	9	0	0
SM + Z' ($m_{Z'} = 3$ TeV)	26500 ± 400	1490 ± 60	214 ± 11	48.4 ± 3.2	19.0 ± 1.6	6.0 ± 0.6	2.3 ± 0.5	0.9 ± 0.5
SM + CI ($\Delta_{LL}^{\text{Const.}} = 20$ TeV)	26500 ± 400	1500 ± 60	220 ± 11	52.1 ± 3.2	22.2 ± 1.6	8.8 ± 0.6	2.22 ± 0.14	0.289 ± 0.018
$m_{\mu\mu}$ [GeV]	120–300	300–500	500–700	700–900	900–1200	1200–1800	1800–3000	3000–6000
Drell–Yan (Z/γ^*)	19300 ± 400	770 ± 31	115 ± 7	29.0 ± 2.2	11.8 ± 1.0	4.0 ± 0.4	0.61 ± 0.09	0.034 ± 0.007
Top quarks	3855 ± 29	369 ± 9	43.4 ± 2.5	7.5 ± 0.5	1.97 ± 0.16	0.36 ± 0.04	0.020 ± 0.004	< 0.001
Diboson	412.1 ± 3.4	43.7 ± 0.9	7.08 ± 0.30	1.67 ± 0.11	0.61 ± 0.05	0.174 ± 0.023	0.020 ± 0.006	< 0.001
Total SM	23600 ± 400	1183 ± 32	165 ± 7	38.1 ± 2.2	14.4 ± 1.0	4.6 ± 0.4	0.65 ± 0.09	0.036 ± 0.008
Data	23275	1083	164	29	13	5	0	0
SM + Z' ($m_{Z'} = 3$ TeV)	23600 ± 400	1183 ± 32	165 ± 7	38.1 ± 2.2	14.4 ± 1.0	4.6 ± 0.4	1.27 ± 0.12	0.55 ± 0.09
SM + CI ($\Delta_{LL}^{\text{Const.}} = 20$ TeV)	23600 ± 400	1193 ± 32	174 ± 8	41.9 ± 2.4	16.8 ± 1.2	6.4 ± 0.6	1.49 ± 0.20	0.164 ± 0.028

The uncertainty in the electron identification efficiency extrapolation is based on the differences in the electron shower shapes in the EM calorimeters between data and MC simulation in the $Z \rightarrow ee$ peak, which are propagated to the high- E_T electron sample. The effect on the electron identification efficiency was found to be 2.0% and is independent of E_T for electrons with E_T above 150 GeV. Mismodelling of the muon momentum resolution due to residual misalignments in the MS can alter the steeply falling background shape at high dilepton mass and can significantly modify the width of the signal line shape. This uncertainty is obtained by studying dedicated data-taking periods with no magnetic field in the MS [45]. For the dielectron channel, the uncertainty includes a contribution from the multi-jet and W + jets data-driven estimate that is obtained by varying both the overall normalisation and the extrapolation methodology, which is explained in Section 5. Systematic uncertainties used in the statistical analysis of the results are summarised in Table 1 at dilepton mass values of 2 TeV and 3 TeV.

7. Event yields

Expected and observed event yields, in bins of invariant mass, are shown in Table 2 for the dielectron (top) and dimuon (bottom) channels. Expected event yields are split into the different background sources and the yields for two signal scenarios. The DY process is dominant over the entire mass range. In general, the observed data are in good agreement with the SM prediction, taking uncertainties into account as described in Section 6. A deficit is observed for the dimuon channel in the invariant mass region between 300 GeV and 500 GeV. Extensive cross-checks were performed in this region, and the deficit was quantified by calculating the local Poisson p -value, using the sources of systematic uncertainty described in Section 6, which gives a significance less than two standard deviations for this mass interval.

Distributions of $m_{\ell\ell}$ in the dielectron and dimuon channels are shown in Fig. 1. No significant excess is observed. The highest invariant mass event is found at 1775 GeV in the dielectron channel, and 1587 GeV in the dimuon channel. Both of these events appear

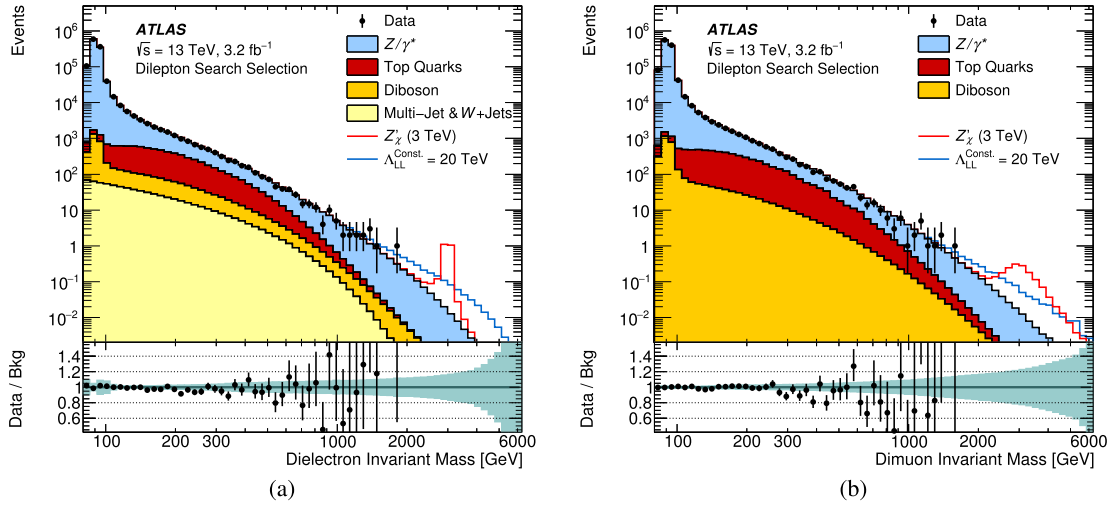


Fig. 1. Distributions of (a) dielectron and (b) dimuon reconstructed invariant mass ($m_{\ell\ell}$) after selection, for data and the SM background estimates as well as their ratio. Two selected signals are overlaid; resonant Z'_χ with a pole mass of 3 TeV and non-resonant contact interactions with left–left (LL) constructive interference and $\Lambda = 20$ TeV. The bin width of the distributions is constant in $\log(m_{\ell\ell})$, and the shaded band in the lower panel illustrates the total systematic uncertainty, as explained in Section 6. The data points are shown together with their statistical uncertainty.

to be very clean with little other detector activity, apart from an accompanying jet in the dimuon event.

8. Statistical analysis

A search for a resonant signal is performed using the $m_{\ell\ell}$ distribution in the dielectron and dimuon channels utilising the log-likelihood ratio (LLR) test described in Ref. [51]. To perform the LLR search, the HistFactory [52] package, together with RooStats [53] and RooFit [54] packages are used. The p -value for finding a Z'_χ signal excess (at a given pole mass) more significant than the observed, is computed analytically using a test statistic based on the logarithm of the profile likelihood ratio $\lambda(\mu)$ which includes a treatment of the systematic uncertainties. The parameter μ is defined as a ratio of the signal production cross-section times branching ratio to the dilepton final state (σB) to its theoretically predicted value. The test statistic is modified for signal masses below 800 GeV to also quantify the significance of potential deficits in the data. The analytical calculation of p -values is cross-checked using MC simulations. Multiple mass hypotheses are tested in pole-mass steps corresponding to the histogram bin width to compute the local p -values – that is p -values corresponding to specific signal mass hypotheses. The chosen bin width for the $m_{\ell\ell}$ histogram corresponds to the resolution in the dielectron (dimuon) channel, which varies from 10 (60) GeV at $m_{\ell\ell} = 1$ TeV to 15 (200) GeV at $m_{\ell\ell} = 2$ TeV, and 20 (420) GeV at $m_{\ell\ell} = 3$ TeV. Pseudo-experiments are used to estimate the distribution of the lowest local p -value in the absence of any signal. The p -value to find anywhere in the $m_{\ell\ell}$ distribution (120–6000 GeV) an excess more significant than the one in the data (global p -value) is then computed. The BUMPHUNTER method [55] is also used in a model-independent search for an excess in all consecutive intervals in the $m_{\ell\ell}$ histogram spanning from one bin to half of the bins in the histogram. The same binning as in the LLR search is used.

Upper limits on the Z' σB and lower limits on the CI scale Λ in a variety of interference and chiral coupling scenarios are set in a Bayesian approach. The logarithmic $m_{\ell\ell}$ histogram binning shown in Fig. 1 uses 66 mass bins and is chosen for setting limits on resonant signals using Z'_χ signal templates. For setting the limits on the CI interaction scale Λ , the $m_{\ell\ell}$ mass distribution uses eight mass bins above 400 GeV with bin widths varying from 100 to 1500 GeV. The prior probability is chosen to be uniform and

positive in the cross-section for the Z' limit calculation and $1/\Lambda^2$ or $1/\Lambda^4$ for the CI limit calculation. For the CI limit calculation, these choices of the prior are selected to study the cases where the dilepton production cross-section is dominated by the interference terms and where it is dominated by the pure contact interaction term. The upper (lower) 95% percentile of the posterior probability is then quoted as the upper (lower) 95% credibility-level limit on σB (Λ). The above calculations are performed with the Bayesian Analysis Toolkit (BAT) [56], which uses a Markov Chain MC technique to integrate over the nuisance parameters. Limit values obtained using the experimental data are quoted as observed limits, while median values of the limits from a large number of pseudo-experiments, where only SM background is present, are quoted as the expected limits. The upper limits on the σB in a Z' model are interpreted as lower limits on the Z' pole mass using the relationship between the pole mass and the theoretical Z' cross-section.

9. Results

The statistical tests described in the previous section do not reveal a signal. The LLR tests for a Z'_χ find global p -values of 88%, 26% and 89% in the dielectron, dimuon, and combined channels, respectively. The BUMPHUNTER [55] test, which scans the mass spectrum with varying intervals to find the most significant excess in data, finds p -values of 41% and 78% in the dielectron and dimuon channels, respectively. The largest deviation from the background-only hypothesis using the LLR tests for a Z'_χ is observed at 192 GeV in the dimuon mass spectrum with a local significance of 2.5σ , but is not globally significant (0.6σ). There are also smaller but noticeable excesses in dimuon channel at 583 GeV with a local significance of 1.8σ , in the dielectron channel at 652 GeV with a local significance of 2.0σ , and in the combined dilepton channel at 1410 GeV with a local significance of 2.0σ . Upper limits on the cross-section times branching ratio (σB) for Z' bosons are presented in Fig. 2(a). The observed and expected lower pole-mass limits for various Z' scenarios are summarised in Table 3. The upper limits on σB for Z' bosons start to weaken above a pole mass of ~ 3 TeV. This is mainly due to the combined effect of a rapidly-falling signal cross-section as the kinematic limit is approached, and the natural width of the resonance. The effect is more pronounced in the dimuon channel due to worse mass resolution than in the dielectron channel. The selection efficiency also

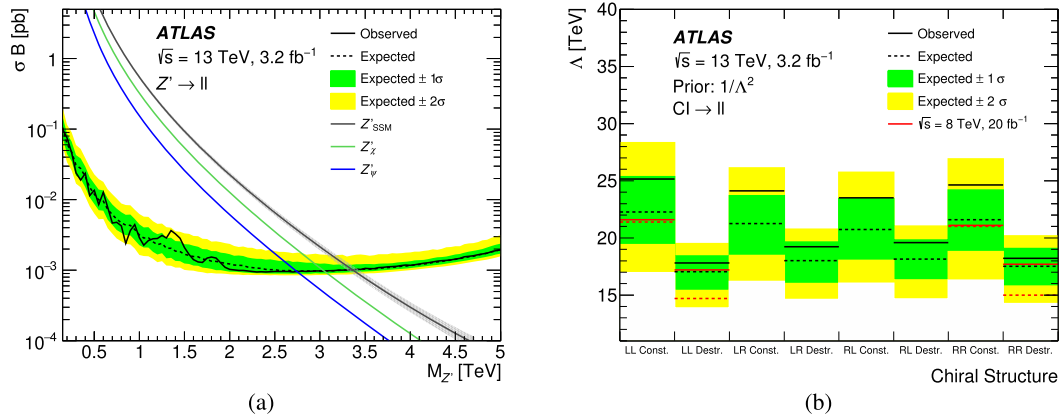


Fig. 2. (a) Upper 95% CL limits for Z' production cross-section times branching ratio to two leptons as a function of Z' pole mass ($M_{Z'}$). The signal theory lines are calculated with PYTHIA 8 using the NNPDF23LO PDF set [38], and corrected to next-to-next-to-leading order in QCD using VRAP [25] and the CT14NNLO PDF set [26]. The signal theoretical uncertainties are shown as a band on the Z'_{SSM} theory line for illustration purposes, but are not included in the σB limit calculation. (b) Lower 95% CL limits on the contact interaction (CI) scale Λ for different chiral couplings and both constructive and destructive interference scenarios using a uniform positive prior in $1/\Lambda^2$. For the left-left (LL) and right-right (RR) cases, the ATLAS $\sqrt{s} = 8$ TeV results [12] are shown for comparison. In that publication, the left-right (LR) case was obtained by setting $\eta_{LR} = \eta_{RL} = \pm 1$ and therefore is not directly comparable to the results presented here.

Table 3

Observed and expected 95% CL lower mass limits for various Z' gauge boson models. The widths are quoted as a percentage of the resonance mass.

Model	Width [%]	θ_{E_6} [rad]	Lower limits on $m_{Z'}$ [TeV]					
			ee		$\mu\mu$		$\ell\ell$	
			Obs.	Exp.	Obs.	Exp.	Obs.	Exp.
Z'_{SSM}	3.0	–	3.17	3.16	2.83	2.89	3.36	3.36
Z'_χ	1.2	0.50π	2.87	2.86	2.57	2.60	3.05	3.05
Z'_S	1.2	0.63π	2.83	2.81	2.54	2.57	3.00	3.00
Z'_I	1.1	0.71π	2.77	2.76	2.49	2.51	2.94	2.94
Z'_η	0.6	0.21π	2.63	2.62	2.35	2.36	2.81	2.80
Z'_N	0.6	-0.08π	2.63	2.62	2.35	2.36	2.80	2.80
Z'_ψ	0.5	0	2.57	2.55	2.29	2.29	2.74	2.74

Table 4

Observed and expected 95% CL lower limits on Λ for the LL, LR, RL, and RR chiral coupling scenarios, for both the constructive and destructive interference cases using a uniform positive prior in $1/\Lambda^2$ or $1/\Lambda^4$. The dielectron, dimuon, and combined dilepton channel limits are shown.

Channel	Prior	Lower limits on Λ [TeV]							
		Left–Left		Left–Right		Right–Left		Right–Right	
		Const.	Destr.	Const.	Destr.	Const.	Destr.	Const.	Destr.
Obs.: ee	$1/\Lambda^2$	19.5	15.5	18.7	16.2	18.5	16.4	18.5	16.4
Exp.: ee	$1/\Lambda^2$	19.5	15.8	18.7	16.5	18.4	16.5	18.4	16.6
Obs.: ee	$1/\Lambda^4$	17.7	14.4	17.0	15.0	16.8	15.1	16.8	15.1
Exp.: ee	$1/\Lambda^4$	17.6	14.7	16.9	15.3	16.8	15.3	16.8	15.4
Obs.: $\mu\mu$	$1/\Lambda^2$	21.8	15.8	21.1	16.9	20.5	17.2	22.0	15.7
Exp.: $\mu\mu$	$1/\Lambda^2$	17.9	14.5	17.4	15.2	17.2	15.3	17.9	14.5
Obs.: $\mu\mu$	$1/\Lambda^4$	19.0	14.9	18.5	15.7	18.1	15.9	19.1	14.8
Exp.: $\mu\mu$	$1/\Lambda^4$	16.5	13.9	16.1	14.5	15.9	14.5	16.7	13.9
Obs.: $\ell\ell$	$1/\Lambda^2$	25.2	17.8	24.1	19.2	23.5	19.6	24.6	18.2
Exp.: $\ell\ell$	$1/\Lambda^2$	22.3	17.0	21.3	18.0	20.7	18.1	21.6	17.5
Obs.: $\ell\ell$	$1/\Lambda^4$	22.2	16.7	21.3	17.8	21.0	18.1	21.7	17.0
Exp.: $\ell\ell$	$1/\Lambda^4$	20.2	15.9	19.6	17.0	19.1	17.0	19.5	16.5

starts to slowly decrease at very high pole mass, but this is a subdominant effect. The lower limits on the CI scale, Λ , where a prior uniform and positive in $1/\Lambda^2$ is used are summarised in Fig. 2(b). Table 4 gives an overview of Λ lower limits for all considered chiral coupling and interference scenarios as well as both choices of the prior Λ probability.

10. Conclusions

The ATLAS detector at the Large Hadron Collider has been used to search for resonant and non-resonant new phenomena in the

dilepton invariant mass spectrum above the Z -boson pole. The search is conducted with 3.2 fb^{-1} of pp collision data at $\sqrt{s} = 13 \text{ TeV}$, recorded during 2015. The highest invariant mass event is found at 1775 GeV in the dielectron channel, and 1587 GeV in the dimuon channel. The observed dilepton invariant mass spectrum is consistent with the Standard Model prediction, within systematic and statistical uncertainties. Among a choice of different models, the data are interpreted in terms of resonant spin-1 Z' gauge boson production and non-resonant contact interactions. Upper limits are therefore set on the cross-section times branching

ratio for a spin-1 Z' gauge boson. The resulting lower mass limits are 3.36 TeV for the Z'_{SSM} , 3.05 TeV for the Z'_χ , and 2.74 TeV for the Z'_ψ . Other E_6 Z' models are also constrained in the range between those quoted for the Z'_χ and Z'_ψ . These are more stringent than the previous ATLAS result obtained at $\sqrt{s} = 8$ TeV, by up to 450 GeV. The lower limits on the energy scale Λ for various $\ell\ell qq$ contact interaction models range between 16.7 TeV and 25.2 TeV, which are more stringent than the previous ATLAS result obtained at $\sqrt{s} = 8$ TeV, by up to 3.6 TeV.

Acknowledgements

We thank CERN for the very successful operation of the LHC, as well as the support staff from our institutions without whom ATLAS could not be operated efficiently.

We acknowledge the support of ANPCyT, Argentina; YerPhI, Armenia; ARC, Australia; BMWFW and FWF, Austria; ANAS, Azerbaijan; SSTC, Belarus; CNPq and FAPESP, Brazil; NSERC, NRC and CFI, Canada; CERN; CONICYT, Chile; CAS, MOST and NSFC, China; COLCIENCIAS, Colombia; MSMT CR, MPO CR and VSC CR, Czech Republic; DNRF and DNSRC, Denmark; IN2P3-CNRS, CEA-DSM/IRFU, France; GNSF, Georgia; BMBF, HGF, and MPG, Germany; GSRT, Greece; RGC, Hong Kong SAR, China; ISF, I-CORE and Benoziyo Center, Israel; INFN, Italy; MEXT and JSPS, Japan; CNRST, Morocco; FOM and NWO, Netherlands; RCN, Norway; MNiSW and NCN, Poland; FCT, Portugal; MNE/IFA, Romania; MES of Russia and NRC KI, Russian Federation; JINR; MESTD, Serbia; MSSR, Slovakia; ARRS and MIZŠ, Slovenia; DST/NRF, South Africa; MINECO, Spain; SRC and Knut and Alice Wallenberg Foundation, Sweden; SERI, SNSF and Cantons of Bern and Geneva, Switzerland; MOST, Taiwan; TAEK, Turkey; STFC, United Kingdom; DOE and NSF, United States. In addition, individual groups and members have received support from BCKDF, the Canada Council, CANARIE, CRC, Compute Canada, FQRNT, and the Ontario Innovation Trust, Canada; EPLANET, ERC, FP7, Horizon 2020 and Marie Skłodowska-Curie Actions, European Union; Investissements d'Avenir Labex and Idex, ANR, Région Auvergne and Fondation Partager le Savoir, France; DFG and AvH Foundation, Germany; Herakleitos, Thales and Aristeia programmes co-financed by EU-ESF and the Greek NSRF; BSF, GIF and Minerva, Israel; BRF, Norway; Generalitat de Catalunya, Generalitat Valenciana, Spain; the Royal Society and Leverhulme Trust, United Kingdom.

The crucial computing support from all WLCG partners is acknowledged gratefully, in particular from CERN, the ATLAS Tier-1 facilities at TRIUMF (Canada), NDGF (Denmark, Norway, Sweden), CC-IN2P3 (France), KIT/GridKA (Germany), INFN-CNAF (Italy), NL-T1 (Netherlands), PIC (Spain), ASGC (Taiwan), RAL (UK) and BNL (USA), the Tier-2 facilities worldwide and large non-WLCG resource providers. Major contributors of computing resources are listed in Ref. [57].

References

- [1] D. London, J.L. Rosner, Extra gauge bosons in $E(6)$, *Phys. Rev. D* 34 (1986) 1530.
- [2] P. Langacker, The physics of heavy Z' gauge bosons, *Rev. Mod. Phys.* 81 (2009) 1199–1228, arXiv:0801.1345 [hep-ph].
- [3] L. Randall, R. Sundrum, A large mass hierarchy from a small extra dimension, *Phys. Rev. Lett.* 83 (1999) 3370–3373, arXiv:hep-ph/9905221.
- [4] P. Meade, L. Randall, Black holes and quantum gravity at the LHC, *J. High Energy Phys.* 05 (2008) 003, arXiv:0708.3017 [hep-ph].
- [5] M.V. Chizhov, V.A. Bednyakov, J.A. Budagov, Proposal for chiral bosons search at LHC via their unique new signature, *Phys. At. Nucl.* 71 (2008) 2096–2100, arXiv:0801.4235 [hep-ph].
- [6] F. Sannino, K. Tuominen, Orientifold theory dynamics and symmetry breaking, *Phys. Rev. D* 71 (2005) 051901, arXiv:hep-ph/0405209.
- [7] E. Eichten, K.D. Lane, M.E. Peskin, New tests for quark and lepton substructure, *Phys. Rev. Lett.* 50 (1983) 811–814.
- [8] E. Eichten, et al., Super collider physics, *Rev. Mod. Phys.* 56 (1984) 579–707.
- [9] N. Arkani-Hamed, S. Dimopoulos, G.R. Dvali, Phenomenology, astrophysics and cosmology of theories with submillimeter dimensions and TeV scale quantum gravity, *Phys. Rev. D* 59 (1999) 086004, arXiv:hep-ph/9807344.
- [10] ATLAS Collaboration, Search for high-mass dilepton resonances in pp collisions at $\sqrt{s} = 8$ TeV with the ATLAS detector, *Phys. Rev. D* 90 (2014) 052005, arXiv:1405.4123 [hep-ex].
- [11] CMS Collaboration, Search for physics beyond the standard model in dilepton mass spectra in proton–proton collisions at $\sqrt{s} = 8$ TeV, *J. High Energy Phys.* 04 (2015) 025, arXiv:1412.6302 [hep-ex].
- [12] ATLAS Collaboration, Search for contact interactions and large extra dimensions in the dilepton channel using proton–proton collisions at $\sqrt{s} = 8$ TeV with the ATLAS detector, *Eur. Phys. J. C* 74 (2014) 3134, arXiv:1407.2410 [hep-ex].
- [13] ATLAS Collaboration, The ATLAS experiment at the CERN large hadron collider, *J. Instrum.* 3 (2008) S08003.
- [14] ATLAS Collaboration, ATLAS insertable B-layer technical design report, ATLAS-TDR-19, 2010, <http://cds.cern.ch/record/1291633>; ATLAS Collaboration, ATLAS insertable B-layer technical design report, ATLAS-TDR-19-ADD-1, 2012, <http://cds.cern.ch/record/1451888> (Addendum).
- [15] ATLAS Collaboration, Monte Carlo generators for the production of a W or Z/γ^* boson in association with jets at ATLAS in Run 2, <http://cds.cern.ch/record/2120133>, 2016.
- [16] ATLAS Collaboration, Simulation of top quark production for the ATLAS experiment at $\sqrt{s} = 13$ TeV, <http://cds.cern.ch/record/2120417>, 2016.
- [17] ATLAS Collaboration, Multi-boson simulation for 13 TeV ATLAS analyses, <http://cds.cern.ch/record/2119986>, 2016.
- [18] S. Alioli, et al., A general framework for implementing NLO calculations in shower Monte Carlo programs: the POWHEG BOX, *J. High Energy Phys.* 06 (2010) 043, arXiv:1002.2581 [hep-ex].
- [19] T. Sjöstrand, S. Mrenna, P.Z. Skands, A brief introduction to PYTHIA 8.1, *Comput. Phys. Commun.* 178 (2008) 852–867, arXiv:0710.3820 [hep-ph].
- [20] H.-L. Lai, et al., New parton distributions for collider physics, *Phys. Rev. D* 82 (2010) 074024, arXiv:1007.2241 [hep-ph].
- [21] ATLAS Collaboration, Measurement of the Z/γ^* boson transverse momentum distribution in pp collisions at $\sqrt{s} = 7$ TeV with the ATLAS detector, *J. High Energy Phys.* 09 (2014) 55, arXiv:1406.3660 [hep-ex].
- [22] J. Pumplin, et al., New generation of parton distributions with uncertainties from global QCD analysis, *J. High Energy Phys.* 07 (2002) 012, arXiv:hep-ph/0201195.
- [23] D.J. Lange, The EvtGen particle decay simulation package, *Nucl. Instrum. Methods A* 462 (2001) 152.
- [24] N. Davidson, T. Przedzinski, Z. Was, PHOTOS interface in C++: technical and physics documentation, *Comput. Phys. Commun.* 199 (2016) 86–101, arXiv:1011.0937 [hep-ph].
- [25] C. Anastasiou, et al., High precision QCD at hadron colliders: electroweak gauge boson rapidity distributions at NNLO, *Phys. Rev. D* 69 (2004) 094008, arXiv:hep-ph/0312266.
- [26] S. Dulat, et al., New parton distribution functions from a global analysis of quantum chromodynamics, *Phys. Rev. D* 93 (2016) 033006, arXiv:1506.07443 [hep-ph].
- [27] S.G. Bondarenko, A.A. Sapronov, NLO EW and QCD proton–proton cross section calculations with mcsanc-v1.01, *Comput. Phys. Commun.* 184 (2013) 2343–2350, arXiv:1301.3687 [hep-ph].
- [28] A.D. Martin, et al., Parton distributions incorporating QED contributions, *Eur. Phys. J. C* 39 (2005) 155–161, arXiv:hep-ph/0411040.
- [29] T. Gleisberg, et al., Event generation with SHERPA 1.1, *J. High Energy Phys.* 02 (2009) 007, arXiv:0811.4622 [hep-ph].
- [30] T. Gleisberg, S. Höche, Comix, a new matrix element generator, *J. High Energy Phys.* 12 (2008) 039, arXiv:0808.3674 [hep-ph].
- [31] F. Cascioli, P. Maierhofer, S. Pozzorini, Scattering amplitudes with open loops, *Phys. Rev. Lett.* 108 (2012) 111601, arXiv:1111.5206 [hep-ph].
- [32] S. Schumann, F. Krauss, A parton shower algorithm based on Catani–Seymour dipole factorisation, *J. High Energy Phys.* 03 (2008) 038, arXiv:0709.1027 [hep-ph].
- [33] S. Höche, et al., QCD matrix elements + parton showers: the NLO case, *J. High Energy Phys.* 04 (2013) 027, arXiv:1207.5030 [hep-ph].
- [34] P. Artoisenet, et al., Automatic spin-entangled decays of heavy resonances in Monte Carlo simulations, *J. High Energy Phys.* 03 (2013) 015, arXiv:1212.3460 [hep-ph].
- [35] T. Sjöstrand, S. Mrenna, P.Z. Skands, PYTHIA 6.4 physics and manual, *J. High Energy Phys.* 05 (2006) 026, arXiv:hep-ph/0603175.
- [36] P.Z. Skands, Tuning Monte Carlo generators: the Perugia tunes, *Phys. Rev. D* 82 (2010) 074018, arXiv:1005.3457 [hep-ph].
- [37] M. Czakon, A. Mitov, Top++: a program for the calculation of the top-pair cross-section at hadron colliders, *Comput. Phys. Commun.* 185 (2014) 2930, arXiv:1112.5675 [hep-ph].
- [38] R.D. Ball, et al., Parton distributions with LHC data, *Nucl. Phys. B* 867 (2013) 244–289, arXiv:1207.1303 [hep-ph].

- [39] ATLAS Collaboration, ATLAS Pythia 8 tunes to 7 TeV data, ATL-PHYS-PUB-2014-021, <http://cds.cern.ch/record/1966419>, 2014.
- [40] S. Agostinelli, et al., GEANT4: a simulation toolkit, Nucl. Instrum. Methods A 506 (2003) 250–303.
- [41] ATLAS Collaboration, The ATLAS simulation infrastructure, Eur. Phys. J. C 70 (2010) 823–874, arXiv:1005.4568 [hep-ph].
- [42] ATLAS Collaboration, Electron efficiency measurements with the ATLAS detector using the 2012 LHC proton–proton collision data, ATLAS-CONF-2014-032, <http://cdsweb.cern.ch/record/1706245>, 2014.
- [43] ATLAS Collaboration, Electron efficiency measurements with the ATLAS detector using the 2015 LHC proton–proton collision data, ATLAS-CONF-2016-024, <http://cdsweb.cern.ch/record/2142831>, 2016.
- [44] ATLAS Collaboration, Electron and photon energy calibration with the ATLAS detector using LHC Run 1 data, Eur. Phys. J. C 74 (2014) 3071, arXiv:1407.5063 [hep-ex].
- [45] ATLAS Collaboration, Muon reconstruction performance of the ATLAS detector in proton–proton collision data at $\sqrt{s} = 13$ TeV, Eur. Phys. J. C 76 (2016) 292, arXiv:1603.05598 [hep-ex].
- [46] ATLAS Collaboration, Improved luminosity determination in pp collisions at $\sqrt{s} = 7$ TeV using the ATLAS detector at the LHC, Eur. Phys. J. C 73 (2013) 2518, arXiv:1302.4393 [hep-ex].
- [47] J. Gao, P. Nadolsky, A meta-analysis of parton distribution functions, J. High Energy Phys. 07 (2014) 035, arXiv:1401.0013 [hep-ph].
- [48] J. Butterworth, et al., PDF4LHC recommendations for LHC Run II, J. Phys. G 43 (2016) 023001, arXiv:1510.03865 [hep-ph].
- [49] P. Motylinski, et al., Updates of PDFs for the 2nd LHC run, arXiv:1411.2560 [hep-ph], 2014.
- [50] R.D. Ball, et al., Parton distributions for the LHC Run II, J. High Energy Phys. 04 (2015) 040, arXiv:1410.8849 [hep-ph].
- [51] G. Cowan, et al., Asymptotic formulae for likelihood-based tests of new physics, Eur. Phys. J. C 71 (2011) 1554, arXiv:1007.1727 [physics.data-an], Eur. Phys. J. C 73 (2013) 2501 (Erratum).
- [52] K. Cranmer, et al., HistFactory: a tool for creating statistical models for use with RooFit and RooStats, <http://cds.cern.ch/record/1456844>, 2012.
- [53] L. Moneta, et al., The RooStats project, arXiv:1009.1003 [physics.data-an], 2010.
- [54] W. Verkerke, D.P. Kirkby, The RooFit toolkit for data modeling, arXiv:physics/0306116, 2003.
- [55] G. Choudalakis, On hypothesis testing, trials factor, hypertexts and the Bump-Hunter, arXiv:1101.0390 [physics.data-an], 2011.
- [56] A. Caldwell, D. Kollar, K. Kroninger, BAT: the Bayesian analysis toolkit, Comput. Phys. Commun. 180 (2009) 2197–2209, arXiv:0808.2552 [physics.data-an].
- [57] ATLAS Collaboration, ATLAS computing acknowledgements 2016–2017, <http://cds.cern.ch/record/2202407>, 2016.

ATLAS Collaboration

M. Aaboud^{136d}, G. Aad⁸⁷, B. Abbott¹¹⁴, J. Abdallah⁶⁵, O. Abdinov¹², B. Abeloos¹¹⁸, R. Aben¹⁰⁸, O.S. AbouZeid¹³⁸, N.L. Abraham¹⁵⁰, H. Abramowicz¹⁵⁴, H. Abreu¹⁵³, R. Abreu¹¹⁷, Y. Abulaiti^{147a,147b}, B.S. Acharya^{164a,164b,a}, L. Adamczyk^{40a}, D.L. Adams²⁷, J. Adelman¹⁰⁹, S. Adomeit¹⁰¹, T. Adye¹³², A.A. Affolder⁷⁶, T. Agatonovic-Jovin¹⁴, J. Agricola⁵⁶, J.A. Aguilar-Saavedra^{127a,127f}, S.P. Ahlen²⁴, F. Ahmadov^{67,b}, G. Aielli^{134a,134b}, H. Akerstedt^{147a,147b}, T.P.A. Åkesson⁸³, A.V. Akimov⁹⁷, G.L. Alberghi^{22a,22b}, J. Albert¹⁶⁹, S. Albrand⁵⁷, M.J. Alconada Verzini⁷³, M. Aleksa³², I.N. Aleksandrov⁶⁷, C. Alexa^{28b}, G. Alexander¹⁵⁴, T. Alexopoulos¹⁰, M. Alhroob¹¹⁴, B. Ali¹²⁹, M. Aliev^{75a,75b}, G. Alimonti^{93a}, J. Alison³³, S.P. Alkire³⁷, B.M.M. Allbrooke¹⁵⁰, B.W. Allen¹¹⁷, P.P. Allport¹⁹, A. Aloisio^{105a,105b}, A. Alonso³⁸, F. Alonso⁷³, C. Alpigiani¹³⁹, M. Alstaty⁸⁷, B. Alvarez Gonzalez³², D. Álvarez Piqueras¹⁶⁷, M.G. Alviggi^{105a,105b}, B.T. Amadio¹⁶, K. Amako⁶⁸, Y. Amaral Coutinho^{26a}, C. Amelung²⁵, D. Amidei⁹¹, S.P. Amor Dos Santos^{127a,127c}, A. Amorim^{127a,127b}, S. Amoroso³², G. Amundsen²⁵, C. Anastopoulos¹⁴⁰, L.S. Ancu⁵¹, N. Andari¹⁰⁹, T. Andeen¹¹, C.F. Anders^{60b}, G. Anders³², J.K. Anders⁷⁶, K.J. Anderson³³, A. Andreazza^{93a,93b}, V. Andrei^{60a}, S. Angelidakis⁹, I. Angelozzi¹⁰⁸, P. Anger⁴⁶, A. Angerami³⁷, F. Anghinolfi³², A.V. Anisenkov^{110,c}, N. Anjos¹³, A. Annovi^{125a,125b}, C. Antel^{60a}, M. Antonelli⁴⁹, A. Antonov^{99,*}, F. Anulli^{133a}, M. Aoki⁶⁸, L. Aperio Bella¹⁹, G. Arabidze⁹², Y. Arai⁶⁸, J.P. Araque^{127a}, A.T.H. Arce⁴⁷, F.A. Arduh⁷³, J.-F. Arguin⁹⁶, S. Argyropoulos⁶⁵, M. Arik^{20a}, A.J. Armbruster¹⁴⁴, L.J. Armitage⁷⁸, O. Arnaez³², H. Arnold⁵⁰, M. Arratia³⁰, O. Arslan²³, A. Artamonov⁹⁸, G. Artoni¹²¹, S. Artz⁸⁵, S. Asai¹⁵⁶, N. Asbah⁴⁴, A. Ashkenazi¹⁵⁴, B. Åsman^{147a,147b}, L. Asquith¹⁵⁰, K. Assamagan²⁷, R. Astalos^{145a}, M. Atkinson¹⁶⁶, N.B. Atlay¹⁴², K. Augsten¹²⁹, G. Avolio³², B. Axen¹⁶, M.K. Ayoub¹¹⁸, G. Azeleos^{96,d}, M.A. Baak³², A.E. Baas^{60a}, M.J. Baca¹⁹, H. Bachacou¹³⁷, K. Bachas^{75a,75b}, M. Backes³², M. Backhaus³², P. Bagiachi^{133a,133b}, P. Bagnaia^{133a,133b}, Y. Bai^{35a}, J.T. Baines¹³², O.K. Baker¹⁷⁶, E.M. Baldin^{110,c}, P. Balek¹³⁰, T. Balestri¹⁴⁹, F. Balli¹³⁷, W.K. Balunas¹²³, E. Banas⁴¹, Sw. Banerjee^{173,e}, A.A.E. Bannoura¹⁷⁵, L. Barak³², E.L. Barberio⁹⁰, D. Barberis^{52a,52b}, M. Barbero⁸⁷, T. Barillari¹⁰², T. Barklow¹⁴⁴, N. Barlow³⁰, S.L. Barnes⁸⁶, B.M. Barnett¹³², R.M. Barnett¹⁶, Z. Barnovska⁵, A. Baroncelli^{135a}, G. Barone²⁵, A.J. Barr¹²¹, L. Barranco Navarro¹⁶⁷, F. Barreiro⁸⁴, J. Barreiro Guimarães da Costa^{35a}, R. Bartoldus¹⁴⁴, A.E. Barton⁷⁴, P. Bartos^{145a}, A. Basalae¹²⁴, A. Bassalat¹¹⁸, R.L. Bates⁵⁵, S.J. Batista¹⁵⁹, J.R. Batley³⁰, M. Battaglia¹³⁸, M. Bause^{133a,133b}, F. Bauer¹³⁷, H.S. Bawa^{144,f}, J.B. Beacham¹¹², M.D. Beattie⁷⁴, T. Beau⁸², P.H. Beauchemin¹⁶², P. Bechtel²³, H.P. Beck^{18,g}, K. Becker¹²¹, M. Becker⁸⁵, M. Beckingham¹⁷⁰, C. Becot¹¹¹, A.J. Beddall^{20e}, A. Beddall^{20b}, V.A. Bednyakov⁶⁷, M. Bedognetti¹⁰⁸, C.P. Bee¹⁴⁹, L.J. Beemster¹⁰⁸, T.A. Beermann³², M. Begel²⁷, J.K. Behr⁴⁴, C. Belanger-Champagne⁸⁹, A.S. Bell⁸⁰, G. Bella¹⁵⁴, L. Bellagamba^{22a}, A. Bellerive³¹, M. Bellomo⁸⁸, K. Belotskiy⁹⁹, O. Beltramello³², N.L. Belyaev⁹⁹, O. Benary¹⁵⁴, D. Benchekroun^{136a}, M. Bender¹⁰¹, K. Bendtz^{147a,147b}, N. Benekos¹⁰, Y. Benhammou¹⁵⁴, E. Benhar Noccioli¹⁷⁶, J. Benitez⁶⁵, D.P. Benjamin⁴⁷, J.R. Bensinger²⁵, S. Bentvelsen¹⁰⁸, L. Beresford¹²¹, M. Beretta⁴⁹, D. Berge¹⁰⁸, E. Bergeas Kuutmann¹⁶⁵, N. Berger⁵, J. Beringer¹⁶, S. Berlendis⁵⁷, N.R. Bernard⁸⁸, C. Bernius¹¹¹,

F.U. Bernlochner²³, T. Berry⁷⁹, P. Berta¹³⁰, C. Bertella⁸⁵, G. Bertoli^{147a,147b}, F. Bertolucci^{125a,125b}, I.A. Bertram⁷⁴, C. Bertsche⁴⁴, D. Bertsche¹¹⁴, G.J. Besjes³⁸, O. Bessidskaia Bylund^{147a,147b}, M. Bessner⁴⁴, N. Besson¹³⁷, C. Betancourt⁵⁰, S. Bethke¹⁰², A.J. Bevan⁷⁸, W. Bhimji¹⁶, R.M. Bianchi¹²⁶, L. Bianchini²⁵, M. Bianco³², O. Biebel¹⁰¹, D. Biedermann¹⁷, R. Bielski⁸⁶, N.V. Biesuz^{125a,125b}, M. Biglietti^{135a}, J. Bilbao De Mendizabal⁵¹, H. Bilokon⁴⁹, M. Bindi⁵⁶, S. Binet¹¹⁸, A. Bingul^{20b}, C. Bini^{133a,133b}, S. Biondi^{22a,22b}, D.M. Bjergaard⁴⁷, C.W. Black¹⁵¹, J.E. Black¹⁴⁴, K.M. Black²⁴, D. Blackburn¹³⁹, R.E. Blair⁶, J.-B. Blanchard¹³⁷, J.E. Blanco⁷⁹, T. Blazek^{145a}, I. Bloch⁴⁴, C. Blocker²⁵, W. Blum^{85,*}, U. Blumenschein⁵⁶, S. Blunier^{34a}, G.J. Bobbink¹⁰⁸, V.S. Bobrovnikov^{110,c}, S.S. Bocchetta⁸³, A. Bocci⁴⁷, C. Bock¹⁰¹, M. Boehler⁵⁰, D. Boerner¹⁷⁵, J.A. Bogaerts³², D. Bogavac¹⁴, A.G. Bogdanchikov¹¹⁰, C. Bohm^{147a}, V. Boisvert⁷⁹, P. Bokan¹⁴, T. Bold^{40a}, A.S. Boldyrev^{164a,164c}, M. Bomben⁸², M. Bona⁷⁸, M. Boonekamp¹³⁷, A. Borisov¹³¹, G. Borissov⁷⁴, J. Bortfeldt³², D. Bortoletto¹²¹, V. Bortolotto^{62a,62b,62c}, K. Bos¹⁰⁸, D. Boscherini^{22a}, M. Bosman¹³, J.D. Bossio Sola²⁹, J. Boudreau¹²⁶, J. Bouffard², E.V. Bouhova-Thacker⁷⁴, D. Boumediene³⁶, C. Bourdarios¹¹⁸, S.K. Boutle⁵⁵, A. Boveia³², J. Boyd³², I.R. Boyko⁶⁷, J. Bracinik¹⁹, A. Brandt⁸, G. Brandt⁵⁶, O. Brandt^{60a}, U. Bratzler¹⁵⁷, B. Brau⁸⁸, J.E. Brau¹¹⁷, H.M. Braun^{175,*}, W.D. Breaden Madden⁵⁵, K. Brendlinger¹²³, A.J. Brennan⁹⁰, L. Brenner¹⁰⁸, R. Brenner¹⁶⁵, S. Bressler¹⁷², T.M. Bristow⁴⁸, D. Britton⁵⁵, D. Britzger⁴⁴, F.M. Brochu³⁰, I. Brock²³, R. Brock⁹², G. Brooijmans³⁷, T. Brooks⁷⁹, W.K. Brooks^{34b}, J. Brosamer¹⁶, E. Brost¹¹⁷, J.H. Broughton¹⁹, P.A. Bruckman de Renstrom⁴¹, D. Bruncko^{145b}, R. Bruneliere⁵⁰, A. Bruni^{22a}, G. Bruni^{22a}, L.S. Bruni¹⁰⁸, B.H. Brunt³⁰, M. Bruschi^{22a}, N. Bruscinò²³, P. Bryant³³, L. Bryngemark⁸³, T. Buanes¹⁵, Q. Buat¹⁴³, P. Buchholz¹⁴², A.G. Buckley⁵⁵, I.A. Budagov⁶⁷, F. Buehrer⁵⁰, M.K. Bugge¹²⁰, O. Bulekov⁹⁹, D. Bullock⁸, H. Burckhart³², S. Burdin⁷⁶, C.D. Burgard⁵⁰, B. Burghgrave¹⁰⁹, K. Burka⁴¹, S. Burke¹³², I. Burmeister⁴⁵, J.T.P. Burr¹²¹, E. Busato³⁶, D. Büscher⁵⁰, V. Büscher⁸⁵, P. Bussey⁵⁵, J.M. Butler²⁴, C.M. Buttar⁵⁵, J.M. Butterworth⁸⁰, P. Butti¹⁰⁸, W. Buttinger²⁷, A. Buzatu⁵⁵, A.R. Buzykaev^{110,c}, S. Cabrera Urbán¹⁶⁷, D. Caforio¹²⁹, V.M. Cairo^{39a,39b}, O. Cakir^{4a}, N. Calace⁵¹, P. Calafiura¹⁶, A. Calandri⁸⁷, G. Calderini⁸², P. Calfayan¹⁰¹, L.P. Caloba^{26a}, S. Calvente Lopez⁸⁴, D. Calvet³⁶, S. Calvet³⁶, T.P. Calvet⁸⁷, R. Camacho Toro³³, S. Camarda³², P. Camarri^{134a,134b}, D. Cameron¹²⁰, R. Caminal Armadans¹⁶⁶, C. Camincher⁵⁷, S. Campana³², M. Campanelli⁸⁰, A. Camplani^{93a,93b}, A. Campoverde¹⁴², V. Canale^{105a,105b}, A. Canepa^{160a}, M. Cano Bret^{35e}, J. Cantero¹¹⁵, R. Cantrill^{127a}, T. Cao⁴², M.D.M. Capeans Garrido³², I. Caprini^{28b}, M. Caprini^{28b}, M. Capua^{39a,39b}, R. Caputo⁸⁵, R.M. Carbone³⁷, R. Cardarelli^{134a}, F. Cardillo⁵⁰, I. Carli¹³⁰, T. Carli³², G. Carlino^{105a}, L. Carminati^{93a,93b}, S. Caron¹⁰⁷, E. Carquin^{34b}, G.D. Carrillo-Montoya³², J.R. Carter³⁰, J. Carvalho^{127a,127c}, D. Casadei¹⁹, M.P. Casado^{13,h}, M. Casolino¹³, D.W. Casper¹⁶³, E. Castaneda-Miranda^{146a}, R. Castelijm¹⁰⁸, A. Castelli¹⁰⁸, V. Castillo Gimenez¹⁶⁷, N.F. Castro^{127a,i}, A. Catinaccio³², J.R. Catmore¹²⁰, A. Cattai³², J. Caudron⁸⁵, V. Cavaliere¹⁶⁶, E. Cavallaro¹³, D. Cavalli^{93a}, M. Cavalli-Sforza¹³, V. Cavasinni^{125a,125b}, F. Ceradini^{135a,135b}, L. Cerda Alberich¹⁶⁷, B.C. Cerio⁴⁷, A.S. Cerqueira^{26b}, A. Cerri¹⁵⁰, L. Cerrito⁷⁸, F. Cerutti¹⁶, M. Cerv³², A. Cervelli¹⁸, S.A. Cetin^{20d}, A. Chafaq^{136a}, D. Chakraborty¹⁰⁹, S.K. Chan⁵⁹, Y.L. Chan^{62a}, P. Chang¹⁶⁶, J.D. Chapman³⁰, D.G. Charlton¹⁹, A. Chatterjee⁵¹, C.C. Chau¹⁵⁹, C.A. Chavez Barajas¹⁵⁰, S. Che¹¹², S. Cheatham⁷⁴, A. Chegwidden⁹², S. Chekanov⁶, S.V. Chekulaev^{160a}, G.A. Chelkov^{67,j}, M.A. Chelstowska⁹¹, C. Chen⁶⁶, H. Chen²⁷, K. Chen¹⁴⁹, S. Chen^{35c}, S. Chen¹⁵⁶, X. Chen^{35f}, Y. Chen⁶⁹, H.C. Cheng⁹¹, H.J. Cheng^{35a}, Y. Cheng³³, A. Cheplakov⁶⁷, E. Cheremushkina¹³¹, R. Cherkaoui El Moursli^{136e}, V. Chernyatin^{27,*}, E. Cheu⁷, L. Chevalier¹³⁷, V. Chiarella⁴⁹, G. Chiarelli^{125a,125b}, G. Chiodini^{75a}, A.S. Chisholm¹⁹, A. Chitan^{28b}, M.V. Chizhov⁶⁷, K. Choi⁶³, A.R. Chomont³⁶, S. Chouridou⁹, B.K.B. Chow¹⁰¹, V. Christodoulou⁸⁰, D. Chromek-Burckhart³², J. Chudoba¹²⁸, A.J. Chuinard⁸⁹, J.J. Chwastowski⁴¹, L. Chytka¹¹⁶, G. Ciapetti^{133a,133b}, A.K. Ciftci^{4a}, D. Cinca⁴⁵, V. Cindro⁷⁷, I.A. Cioara²³, C. Ciocca^{22a,22b}, A. Ciocio¹⁶, F. Ciroto^{105a,105b}, Z.H. Citron¹⁷², M. Citterio^{93a}, M. Ciubancan^{28b}, A. Clark⁵¹, B.L. Clark⁵⁹, M.R. Clark³⁷, P.J. Clark⁴⁸, R.N. Clarke¹⁶, C. Clement^{147a,147b}, Y. Coadou⁸⁷, M. Cobal^{164a,164c}, A. Coccaro⁵¹, J. Cochran⁶⁶, L. Coffey²⁵, L. Colasurdo¹⁰⁷, B. Cole³⁷, A.P. Colijn¹⁰⁸, J. Collot⁵⁷, T. Colombo³², G. Compostella¹⁰², P. Conde Muiño^{127a,127b}, E. Coniavitis⁵⁰, S.H. Connell^{146b}, I.A. Connelly⁷⁹, V. Consorti⁵⁰, S. Constantinescu^{28b}, G. Conti³², F. Conventi^{105a,k}, M. Cooke¹⁶, B.D. Cooper⁸⁰, A.M. Cooper-Sarkar¹²¹, K.J.R. Cormier¹⁵⁹, T. Cornelissen¹⁷⁵, M. Corradi^{133a,133b}, F. Corriveau^{89,l}, A. Corso-Radu¹⁶³, A. Cortes-Gonzalez¹³, G. Cortiana¹⁰², G. Costa^{93a}, M.J. Costa¹⁶⁷, D. Costanzo¹⁴⁰, G. Cottin³⁰,

G. Cowan⁷⁹, B.E. Cox⁸⁶, K. Cranmer¹¹¹, S.J. Crawley⁵⁵, G. Cree³¹, S. Crépé-Renaudin⁵⁷, F. Crescioli⁸², W.A. Cribbs^{147a,147b}, M. Crispin Ortuzar¹²¹, M. Cristinziani²³, V. Croft¹⁰⁷, G. Crosetti^{39a,39b}, T. Cuhadar Donszelmann¹⁴⁰, J. Cummings¹⁷⁶, M. Curatolo⁴⁹, J. Cúth⁸⁵, C. Cuthbert¹⁵¹, H. Czirr¹⁴², P. Czodrowski³, G. D'amen^{22a,22b}, S. D'Auria⁵⁵, M. D'Onofrio⁷⁶, M.J. Da Cunha Sargedas De Sousa^{127a,127b}, C. Da Via⁸⁶, W. Dabrowski^{40a}, T. Dado^{145a}, T. Dai⁹¹, O. Dale¹⁵, F. Dallaire⁹⁶, C. Dallapiccola⁸⁸, M. Dam³⁸, J.R. Dandoy³³, N.P. Dang⁵⁰, A.C. Daniells¹⁹, N.S. Dann⁸⁶, M. Danninger¹⁶⁸, M. Dano Hoffmann¹³⁷, V. Dao⁵⁰, G. Darbo^{52a}, S. Darmora⁸, J. Dassoulas³, A. Dattagupta⁶³, W. Davey²³, C. David¹⁶⁹, T. Davidek¹³⁰, M. Davies¹⁵⁴, P. Davison⁸⁰, E. Dawe⁹⁰, I. Dawson¹⁴⁰, R.K. Daya-Ishmukhametova⁸⁸, K. De⁸, R. de Asmundis^{105a}, A. De Benedetti¹¹⁴, S. De Castro^{22a,22b}, S. De Cecco⁸², N. De Groot¹⁰⁷, P. de Jong¹⁰⁸, H. De la Torre⁸⁴, F. De Lorenzi⁶⁶, A. De Maria⁵⁶, D. De Pedis^{133a}, A. De Salvo^{133a}, U. De Sanctis¹⁵⁰, A. De Santo¹⁵⁰, J.B. De Vivie De Regie¹¹⁸, W.J. Dearnaley⁷⁴, R. Debbe²⁷, C. Debenedetti¹³⁸, D.V. Dedovich⁶⁷, N. Dehghanian³, I. Deigaard¹⁰⁸, M. Del Gaudio^{39a,39b}, J. Del Peso⁸⁴, T. Del Prete^{125a,125b}, D. Delgove¹¹⁸, F. Deliot¹³⁷, C.M. Delitzsch⁵¹, M. Deliyergiyev⁷⁷, A. Dell'Acqua³², L. Dell'Asta²⁴, M. Dell'Orso^{125a,125b}, M. Della Pietra^{105a,k}, D. della Volpe⁵¹, M. Delmastro⁵, P.A. Delsart⁵⁷, D.A. DeMarco¹⁵⁹, S. Demers¹⁷⁶, M. Demichev⁶⁷, A. Demilly⁸², S.P. Denisov¹³¹, D. Denysiuk¹³⁷, D. Derendarz⁴¹, J.E. Derkaoui^{136d}, F. Derue⁸², P. Dervan⁷⁶, K. Desch²³, C. Deterre⁴⁴, K. Dette⁴⁵, P.O. Deviveiros³², A. Dewhurst¹³², S. Dhaliwal²⁵, A. Di Ciaccio^{134a,134b}, L. Di Ciaccio⁵, W.K. Di Clemente¹²³, C. Di Donato^{133a,133b}, A. Di Girolamo³², B. Di Girolamo³², B. Di Micco^{135a,135b}, R. Di Nardo³², A. Di Simone⁵⁰, R. Di Sipio¹⁵⁹, D. Di Valentino³¹, C. Diaconu⁸⁷, M. Diamond¹⁵⁹, F.A. Dias⁴⁸, M.A. Diaz^{34a}, E.B. Diehl⁹¹, J. Dietrich¹⁷, S. Diglio⁸⁷, A. Dimitrievska¹⁴, J. Dingfelder²³, P. Dita^{28b}, S. Dita^{28b}, F. Dittus³², F. Djama⁸⁷, T. Djobava^{53b}, J.I. Djuvsland^{60a}, M.A.B. do Vale^{26c}, D. Dobos³², M. Dobre^{28b}, C. Doglioni⁸³, T. Dohmae¹⁵⁶, J. Dolejsi¹³⁰, Z. Dolezal¹³⁰, B.A. Dolgoshein^{99,*}, M. Donadelli^{26d}, S. Donati^{125a,125b}, P. Dondero^{122a,122b}, J. Donini³⁶, J. Dopke¹³², A. Doria^{105a}, M.T. Dova⁷³, A.T. Doyle⁵⁵, E. Drechsler⁵⁶, M. Dris¹⁰, Y. Du^{35d}, J. Duarte-Campderros¹⁵⁴, E. Duchovni¹⁷², G. Duckeck¹⁰¹, O.A. Ducu^{96,m}, D. Duda¹⁰⁸, A. Dudarev³², E.M. Duffield¹⁶, L. Duflot¹¹⁸, L. Duguid⁷⁹, M. Dührssen³², M. Dumancic¹⁷², M. Dunford^{60a}, H. Duran Yildiz^{4a}, M. Düren⁵⁴, A. Durglishvili^{53b}, D. Duschinger⁴⁶, B. Dutta⁴⁴, M. Dyndal⁴⁴, C. Eckardt⁴⁴, K.M. Ecker¹⁰², R.C. Edgar⁹¹, N.C. Edwards⁴⁸, T. Eifert³², G. Eigen¹⁵, K. Einsweiler¹⁶, T. Ekelof¹⁶⁵, M. El Kacimi^{136c}, V. Ellajosyula⁸⁷, M. Ellert¹⁶⁵, S. Elles⁵, F. Ellinghaus¹⁷⁵, A.A. Elliot¹⁶⁹, N. Ellis³², J. Elmsheuser²⁷, M. Elsing³², D. Emelianov¹³², Y. Enari¹⁵⁶, O.C. Endner⁸⁵, M. Endo¹¹⁹, J.S. Ennis¹⁷⁰, J. Erdmann⁴⁵, A. Ereditato¹⁸, G. Ernis¹⁷⁵, J. Ernst², M. Ernst²⁷, S. Errede¹⁶⁶, E. Ertel⁸⁵, M. Escalier¹¹⁸, H. Esch⁴⁵, C. Escobar¹²⁶, B. Esposito⁴⁹, A.I. Etienvre¹³⁷, E. Etzion¹⁵⁴, H. Evans⁶³, A. Ezhilov¹²⁴, F. Fabbri^{22a,22b}, L. Fabbri^{22a,22b}, G. Facini³³, R.M. Fakhruddinov¹³¹, S. Falciano^{133a}, R.J. Falla⁸⁰, J. Faltova¹³⁰, Y. Fang^{35a}, M. Fanti^{93a,93b}, A. Farbin⁸, A. Farilla^{135a}, C. Farina¹²⁶, E.M. Farina^{122a,122b}, T. Farooque¹³, S. Farrell¹⁶, S.M. Farrington¹⁷⁰, P. Farthouat³², F. Fassi^{136e}, P. Fassnacht³², D. Fassouliotis⁹, M. Fauci Giannelli⁷⁹, A. Favareto^{52a,52b}, W.J. Fawcett¹²¹, L. Fayard¹¹⁸, O.L. Fedin^{124,n}, W. Fedorko¹⁶⁸, S. Feigl¹²⁰, L. Feligioni⁸⁷, C. Feng^{35d}, E.J. Feng³², H. Feng⁹¹, A.B. Fenyuk¹³¹, L. Feremenga⁸, P. Fernandez Martinez¹⁶⁷, S. Fernandez Perez¹³, J. Ferrando⁵⁵, A. Ferrari¹⁶⁵, P. Ferrari¹⁰⁸, R. Ferrari^{122a}, D.E. Ferreira de Lima^{60b}, A. Ferrer¹⁶⁷, D. Ferrere⁵¹, C. Ferretti⁹¹, A. Ferretto Parodi^{52a,52b}, F. Fiedler⁸⁵, A. Filipčić⁷⁷, M. Filipuzzi⁴⁴, F. Filthaut¹⁰⁷, M. Fincke-Keeler¹⁶⁹, K.D. Finelli¹⁵¹, M.C.N. Fiolhais^{127a,127c}, L. Fiorini¹⁶⁷, A. Firan⁴², A. Fischer², C. Fischer¹³, J. Fischer¹⁷⁵, W.C. Fisher⁹², N. Flaschel⁴⁴, I. Fleck¹⁴², P. Fleischmann⁹¹, G.T. Fletcher¹⁴⁰, R.R.M. Fletcher¹²³, T. Flick¹⁷⁵, A. Floderus⁸³, L.R. Flores Castillo^{62a}, M.J. Flowerdew¹⁰², G.T. Forcolin⁸⁶, A. Formica¹³⁷, A. Forti⁸⁶, A.G. Foster¹⁹, D. Fournier¹¹⁸, H. Fox⁷⁴, S. Fracchia¹³, P. Francavilla⁸², M. Franchini^{22a,22b}, D. Francis³², L. Franconi¹²⁰, M. Franklin⁵⁹, M. Frate¹⁶³, M. Fraternali^{122a,122b}, D. Freeborn⁸⁰, S.M. Fressard-Batraneanu³², F. Friedrich⁴⁶, D. Froidevaux³², J.A. Frost¹²¹, C. Fukunaga¹⁵⁷, E. Fullana Torregrosa⁸⁵, T. Fusayasu¹⁰³, J. Fuster¹⁶⁷, C. Gabaldon⁵⁷, O. Gabizon¹⁷⁵, A. Gabrielli^{22a,22b}, A. Gabrielli¹⁶, G.P. Gach^{40a}, S. Gadatsch³², S. Gadomski⁵¹, G. Gagliardi^{52a,52b}, L.G. Gagnon⁹⁶, P. Gagnon⁶³, C. Galea¹⁰⁷, B. Gallardo^{127a,127c}, E.J. Gallas¹²¹, B.J. Gallop¹³², P. Gallus¹²⁹, G. Galster³⁸, K.K. Gan¹¹², J. Gao^{35b,87}, Y. Gao⁴⁸, Y.S. Gao^{144,f}, F.M. Garay Walls⁴⁸, C. García¹⁶⁷, J.E. García Navarro¹⁶⁷, M. Garcia-Sciveres¹⁶, R.W. Gardner³³, N. Garelli¹⁴⁴, V. Garonne¹²⁰, A. Gascon Bravo⁴⁴, C. Gatti⁴⁹, A. Gaudiello^{52a,52b}, G. Gaudio^{122a}, B. Gaur¹⁴², L. Gauthier⁹⁶, I.L. Gavrilenko⁹⁷, C. Gay¹⁶⁸, G. Gaycken²³,

E.N. Gazis¹⁰, Z. Gecse¹⁶⁸, C.N.P. Gee¹³², Ch. Geich-Gimbel²³, M. Geisen⁸⁵, M.P. Geisler^{60a},
 C. Gemme^{52a}, M.H. Genest⁵⁷, C. Geng^{35b,o}, S. Gentile^{133a,133b}, S. George⁷⁹, D. Gerbaudo¹³,
 A. Gershon¹⁵⁴, S. Ghasemi¹⁴², H. Ghazlane^{136b}, M. Ghneimat²³, B. Giacobbe^{22a}, S. Giagu^{133a,133b},
 P. Giannetti^{125a,125b}, B. Gibbard²⁷, S.M. Gibson⁷⁹, M. Gignac¹⁶⁸, M. Gilchriese¹⁶, T.P.S. Gillam³⁰,
 D. Gillberg³¹, G. Gilles¹⁷⁵, D.M. Gingrich^{3,d}, N. Giokaris⁹, M.P. Giordani^{164a,164c}, F.M. Giorgi^{22a},
 F.M. Giorgi¹⁷, P.F. Giraud¹³⁷, P. Giromini⁵⁹, D. Giugni^{93a}, F. Giuli¹²¹, C. Giuliani¹⁰², M. Giulini^{60b},
 B.K. Gjelsten¹²⁰, S. Gkaitatzis¹⁵⁵, I. Gkialas¹⁵⁵, E.L. Gkoukousis¹¹⁸, L.K. Gladilin¹⁰⁰, C. Glasman⁸⁴,
 J. Glatzer⁵⁰, P.C.F. Glaysher⁴⁸, A. Glazov⁴⁴, M. Goblirsch-Kolb¹⁰², J. Godlewski⁴¹, S. Goldfarb⁹⁰,
 T. Golling⁵¹, D. Golubkov¹³¹, A. Gomes^{127a,127b,127d}, R. Gonçalo^{127a},
 J. Goncalves Pinto Firmino Da Costa¹³⁷, G. Gonella⁵⁰, L. Gonella¹⁹, A. Gongadze⁶⁷,
 S. González de la Hoz¹⁶⁷, G. Gonzalez Parra¹³, S. Gonzalez-Sevilla⁵¹, L. Goossens³², P.A. Gorbounov⁹⁸,
 H.A. Gordon²⁷, I. Gorelov¹⁰⁶, B. Gorini³², E. Gorini^{75a,75b}, A. Gorišek⁷⁷, E. Gornicki⁴¹, A.T. Goshaw⁴⁷,
 C. Gössling⁴⁵, M.I. Gostkin⁶⁷, C.R. Goudet¹¹⁸, D. Goujdami^{136c}, A.G. Goussiou¹³⁹, N. Govender^{146b,p},
 E. Gozani¹⁵³, L. Graber⁵⁶, I. Grabowska-Bold^{40a}, P.O.J. Gradin⁵⁷, P. Grafström^{22a,22b}, J. Gramling⁵¹,
 E. Gramstad¹²⁰, S. Grancagnolo¹⁷, V. Gratchev¹²⁴, P.M. Gravila^{28e}, H.M. Gray³², E. Graziani^{135a},
 Z.D. Greenwood^{81,q}, C. Grefe²³, K. Gregersen⁸⁰, I.M. Gregor⁴⁴, P. Grenier¹⁴⁴, K. Grevtsov⁵, J. Griffiths⁸,
 A.A. Grillo¹³⁸, K. Grimm⁷⁴, S. Grinstein^{13,r}, Ph. Gris³⁶, J.-F. Grivaz¹¹⁸, S. Groh⁸⁵, J.P. Grohs⁴⁶,
 E. Gross¹⁷², J. Grosse-Knetter⁵⁶, G.C. Grossi⁸¹, Z.J. Grout¹⁵⁰, L. Guan⁹¹, W. Guan¹⁷³, J. Guenther⁶⁴,
 F. Guescini⁵¹, D. Guest¹⁶³, O. Gueta¹⁵⁴, E. Guido^{52a,52b}, T. Guillemin⁵, S. Guindon², U. Gul⁵⁵,
 C. Gumpert³², J. Guo^{35e}, Y. Guo^{35b,o}, S. Gupta¹²¹, G. Gustavino^{133a,133b}, P. Gutierrez¹¹⁴,
 N.G. Gutierrez Ortiz⁸⁰, C. Gutschow⁴⁶, C. Guyot¹³⁷, C. Gwenlan¹²¹, C.B. Gwilliam⁷⁶, A. Haas¹¹¹,
 C. Haber¹⁶, H.K. Hadavand⁸, N. Haddad^{136e}, A. Hadeef⁸⁷, P. Haefner²³, S. Hageböck²³, Z. Hajduk⁴¹,
 H. Hakobyan^{177,*}, M. Haleem⁴⁴, J. Haley¹¹⁵, G. Halladjian⁹², G.D. Hallewell⁸⁷, K. Hamacher¹⁷⁵,
 P. Hamal¹¹⁶, K. Hamano¹⁶⁹, A. Hamilton^{146a}, G.N. Hamity¹⁴⁰, P.G. Hamnett⁴⁴, L. Han^{35b},
 K. Hanagaki^{68,s}, K. Hanawa¹⁵⁶, M. Hance¹³⁸, B. Haney¹²³, S. Hanisch³², P. Hanke^{60a}, R. Hanna¹³⁷,
 J.B. Hansen³⁸, J.D. Hansen³⁸, M.C. Hansen²³, P.H. Hansen³⁸, K. Hara¹⁶¹, A.S. Hard¹⁷³, T. Harenberg¹⁷⁵,
 F. Hariri¹¹⁸, S. Harkusha⁹⁴, R.D. Harrington⁴⁸, P.F. Harrison¹⁷⁰, F. Hartjes¹⁰⁸, N.M. Hartmann¹⁰¹,
 M. Hasegawa⁶⁹, Y. Hasegawa¹⁴¹, A. Hasib¹¹⁴, S. Hassani¹³⁷, S. Haug¹⁸, R. Hauser⁹², L. Hauswald⁴⁶,
 M. Havranek¹²⁸, C.M. Hawkes¹⁹, R.J. Hawkins³², D. Hayden⁹², C.P. Hays¹²¹, J.M. Hays⁷⁸,
 H.S. Hayward⁷⁶, S.J. Haywood¹³², S.J. Head¹⁹, T. Heck⁸⁵, V. Hedberg⁸³, L. Heelan⁸, S. Heim¹²³,
 T. Heim¹⁶, B. Heinemann¹⁶, J.J. Heinrich¹⁰¹, L. Heinrich¹¹¹, C. Heinz⁵⁴, J. Hejbal¹²⁸, L. Helary²⁴,
 S. Hellman^{147a,147b}, C. Hensens³², J. Henderson¹²¹, R.C.W. Henderson⁷⁴, Y. Heng¹⁷³, S. Henkelmann¹⁶⁸,
 A.M. Henriques Correia³², S. Henrot-Versille¹¹⁸, G.H. Herbert¹⁷, Y. Hernández Jiménez¹⁶⁷, H. Herr⁸⁵,
 G. Herten⁵⁰, R. Hertenberger¹⁰¹, L. Hervas³², G.G. Hesketh⁸⁰, N.P. Hessey¹⁰⁸, J.W. Hetherly⁴²,
 R. Hickling⁷⁸, E. Higón-Rodríguez¹⁶⁷, E. Hill¹⁶⁹, J.C. Hill³⁰, K.H. Hiller⁴⁴, S.J. Hillier¹⁹, I. Hinchliffe¹⁶,
 E. Hines¹²³, R.R. Hinman¹⁶, M. Hirose⁵⁰, D. Hirschbuehl¹⁷⁵, J. Hobbs¹⁴⁹, N. Hod^{160a},
 M.C. Hodgkinson¹⁴⁰, P. Hodgson¹⁴⁰, A. Hoecker³², M.R. Hoferkamp¹⁰⁶, F. Hoenig¹⁰¹, D. Hohn²³,
 T.R. Holmes¹⁶, M. Homann⁴⁵, T.M. Hong¹²⁶, B.H. Hooberman¹⁶⁶, W.H. Hopkins¹¹⁷, Y. Horii¹⁰⁴,
 A.J. Horton¹⁴³, J.-Y. Hostachy⁵⁷, S. Hou¹⁵², A. Hoummada^{136a}, J. Howarth⁴⁴, M. Hrabovsky¹¹⁶,
 I. Hristova¹⁷, J. Hrivnac¹¹⁸, T. Hryn'ova⁵, A. Hrynevich⁹⁵, C. Hsu^{146c}, P.J. Hsu^{152,t}, S.-C. Hsu¹³⁹, D. Hu³⁷,
 Q. Hu^{35b}, Y. Huang⁴⁴, Z. Hubacek¹²⁹, F. Hubaut⁸⁷, F. Huegging²³, T.B. Huffman¹²¹, E.W. Hughes³⁷,
 G. Hughes⁷⁴, M. Huhtinen³², P. Huo¹⁴⁹, N. Huseynov^{67,b}, J. Huston⁹², J. Huth⁵⁹, G. Iacobucci⁵¹,
 G. Iakovidis²⁷, I. Ibragimov¹⁴², L. Iconomidou-Fayard¹¹⁸, E. Ideal¹⁷⁶, Z. Idrissi^{136e}, P. Iengo³²,
 O. Igonkina^{108,u}, T. Iizawa¹⁷¹, Y. Ikegami⁶⁸, M. Ikeno⁶⁸, Y. Ilchenko^{11,v}, D. Iliadis¹⁵⁵, N. Ilic¹⁴⁴,
 T. Ince¹⁰², G. Introzzi^{122a,122b}, P. Ioannou^{9,*}, M. Iodice^{135a}, K. Iordanidou³⁷, V. Ippolito⁵⁹, M. Ishino⁷⁰,
 M. Ishitsuka¹⁵⁸, R. Ishmukhametov¹¹², C. Issever¹²¹, S. Istin^{20a}, F. Ito¹⁶¹, J.M. Iturbe Ponce⁸⁶,
 R. Iuppa^{134a,134b}, W. Iwanski⁴¹, H. Iwasaki⁶⁸, J.M. Izen⁴³, V. Izzo^{105a}, S. Jabbar³, B. Jackson¹²³,
 M. Jackson⁷⁶, P. Jackson¹, V. Jain², K.B. Jakobi⁸⁵, K. Jakobs⁵⁰, S. Jakobsen³², T. Jakoubek¹²⁸,
 D.O. Jamin¹¹⁵, D.K. Jana⁸¹, E. Jansen⁸⁰, R. Jansky⁶⁴, J. Janssen²³, M. Janus⁵⁶, G. Jarlskog⁸³,
 N. Javadov^{67,b}, T. Javůrek⁵⁰, F. Jeanneau¹³⁷, L. Jeanty¹⁶, J. Jejelava^{53a,w}, G.-Y. Jeng¹⁵¹, D. Jennens⁹⁰,
 P. Jenni^{50,x}, J. Jentsch⁴⁵, C. Jeske¹⁷⁰, S. Jézéquel⁵, H. Ji¹⁷³, J. Jia¹⁴⁹, H. Jiang⁶⁶, Y. Jiang^{35b}, S. Jiggins⁸⁰,
 J. Jimenez Pena¹⁶⁷, S. Jin^{35a}, A. Jinaru^{28b}, O. Jinnouchi¹⁵⁸, P. Johansson¹⁴⁰, K.A. Johns⁷, W.J. Johnson¹³⁹,

K. Jon-And ^{147a,147b}, G. Jones ¹⁷⁰, R.W.L. Jones ⁷⁴, S. Jones ⁷, T.J. Jones ⁷⁶, J. Jongmanns ^{60a},
 P.M. Jorge ^{127a,127b}, J. Jovicevic ^{160a}, X. Ju ¹⁷³, A. Juste Rozas ^{13,r}, M.K. Köhler ¹⁷², A. Kaczmarska ⁴¹,
 M. Kado ¹¹⁸, H. Kagan ¹¹², M. Kagan ¹⁴⁴, S.J. Kahn ⁸⁷, E. Kajomovitz ⁴⁷, C.W. Kalderon ¹²¹, A. Kaluza ⁸⁵,
 S. Kama ⁴², A. Kamenshchikov ¹³¹, N. Kanaya ¹⁵⁶, S. Kaneti ³⁰, L. Kanjir ⁷⁷, V.A. Kantserov ⁹⁹, J. Kanzaki ⁶⁸,
 B. Kaplan ¹¹¹, L.S. Kaplan ¹⁷³, A. Kapliy ³³, D. Kar ^{146c}, K. Karakostas ¹⁰, A. Karamaoun ³, N. Karastathis ¹⁰,
 M.J. Kareem ⁵⁶, E. Karentzos ¹⁰, M. Karnevskiy ⁸⁵, S.N. Karpov ⁶⁷, Z.M. Karpova ⁶⁷, K. Karthik ¹¹¹,
 V. Kartvelishvili ⁷⁴, A.N. Karyukhin ¹³¹, K. Kasahara ¹⁶¹, L. Kashif ¹⁷³, R.D. Kass ¹¹², A. Kastanas ¹⁵,
 Y. Kataoka ¹⁵⁶, C. Kato ¹⁵⁶, A. Katre ⁵¹, J. Katzy ⁴⁴, K. Kawagoe ⁷², T. Kawamoto ¹⁵⁶, G. Kawamura ⁵⁶,
 S. Kazama ¹⁵⁶, V.F. Kazanin ^{110,c}, R. Keeler ¹⁶⁹, R. Kehoe ⁴², J.S. Keller ⁴⁴, J.J. Kempster ⁷⁹, K. Kentaro ¹⁰⁴,
 H. Keoshkerian ¹⁵⁹, O. Kepka ¹²⁸, B.P. Kerševan ⁷⁷, S. Kersten ¹⁷⁵, R.A. Keyes ⁸⁹, M. Khader ¹⁶⁶,
 F. Khalil-zada ¹², A. Khanov ¹¹⁵, A.G. Kharlamov ^{110,c}, T.J. Khoo ⁵¹, V. Khovanskiy ⁹⁸, E. Khramov ⁶⁷,
 J. Khubua ^{53b,y}, S. Kido ⁶⁹, H.Y. Kim ⁸, S.H. Kim ¹⁶¹, Y.K. Kim ³³, N. Kimura ¹⁵⁵, O.M. Kind ¹⁷, B.T. King ⁷⁶,
 M. King ¹⁶⁷, S.B. King ¹⁶⁸, J. Kirk ¹³², A.E. Kiryunin ¹⁰², T. Kishimoto ⁶⁹, D. Kisielewska ^{40a}, F. Kiss ⁵⁰,
 K. Kiuchi ¹⁶¹, O. Kivernyk ¹³⁷, E. Kladiva ^{145b}, M.H. Klein ³⁷, M. Klein ⁷⁶, U. Klein ⁷⁶, K. Kleinknecht ⁸⁵,
 P. Klimek ¹⁰⁹, A. Klimentov ²⁷, R. Klingenberg ⁴⁵, J.A. Klinger ¹⁴⁰, T. Klioutchnikova ³², E.-E. Kluge ^{60a},
 P. Kluit ¹⁰⁸, S. Kluth ¹⁰², J. Knapik ⁴¹, E. Kneringer ⁶⁴, E.B.F.G. Knoop ⁸⁷, A. Knue ⁵⁵, A. Kobayashi ¹⁵⁶,
 D. Kobayashi ¹⁵⁸, T. Kobayashi ¹⁵⁶, M. Kobel ⁴⁶, M. Kocian ¹⁴⁴, P. Kodys ¹³⁰, T. Koffas ³¹, E. Koffeman ¹⁰⁸,
 T. Koi ¹⁴⁴, H. Kolanoski ¹⁷, M. Kolb ^{60b}, I. Koletsou ⁵, A.A. Komar ^{97,*}, Y. Komori ¹⁵⁶, T. Kondo ⁶⁸,
 N. Kondrashova ⁴⁴, K. Köneke ⁵⁰, A.C. König ¹⁰⁷, T. Kono ^{68,z}, R. Konoplich ^{111,aa}, N. Konstantinidis ⁸⁰,
 R. Kopeliansky ⁶³, S. Koperny ^{40a}, L. Köpke ⁸⁵, A.K. Kopp ⁵⁰, K. Korcyl ⁴¹, K. Kordas ¹⁵⁵, A. Korn ⁸⁰,
 A.A. Korol ^{110,c}, I. Korolkov ¹³, E.V. Korolkova ¹⁴⁰, O. Kortner ¹⁰², S. Kortner ¹⁰², T. Kosek ¹³⁰,
 V.V. Kostyukhin ²³, A. Kotwal ⁴⁷, A. Kourkouveli-Charalampidi ¹⁵⁵, C. Kourkouvelis ⁹, V. Kouskoura ²⁷,
 A.B. Kowalewska ⁴¹, R. Kowalewski ¹⁶⁹, T.Z. Kowalski ^{40a}, C. Kozakai ¹⁵⁶, W. Kozanecki ¹³⁷, A.S. Kozhin ¹³¹,
 V.A. Kramarenko ¹⁰⁰, G. Kramberger ⁷⁷, D. Krasnopevtsev ⁹⁹, M.W. Krasny ⁸², A. Krasznahorkay ³²,
 J.K. Kraus ²³, A. Kravchenko ²⁷, M. Kretz ^{60c}, J. Kretzschmar ⁷⁶, K. Kreutzfeldt ⁵⁴, P. Krieger ¹⁵⁹, K. Krizka ³³,
 K. Kroeninger ⁴⁵, H. Kroha ¹⁰², J. Kroll ¹²³, J. Kroseberg ²³, J. Krstic ¹⁴, U. Kruchonak ⁶⁷, H. Krüger ²³,
 N. Krumnack ⁶⁶, A. Kruse ¹⁷³, M.C. Kruse ⁴⁷, M. Kruskal ²⁴, T. Kubota ⁹⁰, H. Kucuk ⁸⁰, S. Kuday ^{4b},
 J.T. Kuechler ¹⁷⁵, S. Kuehn ⁵⁰, A. Kugel ^{60c}, F. Kuger ¹⁷⁴, A. Kuhl ¹³⁸, T. Kuhl ⁴⁴, V. Kukhtin ⁶⁷, R. Kukla ¹³⁷,
 Y. Kulchitsky ⁹⁴, S. Kuleshov ^{34b}, M. Kuna ^{133a,133b}, T. Kunigo ⁷⁰, A. Kupco ¹²⁸, H. Kurashige ⁶⁹,
 Y.A. Kurochkin ⁹⁴, V. Kus ¹²⁸, E.S. Kuwertz ¹⁶⁹, M. Kuze ¹⁵⁸, J. Kvita ¹¹⁶, T. Kwan ¹⁶⁹, D. Kyriazopoulos ¹⁴⁰,
 A. La Rosa ¹⁰², J.L. La Rosa Navarro ^{26d}, L. La Rotonda ^{39a,39b}, C. Lacasta ¹⁶⁷, F. Lacava ^{133a,133b}, J. Lacey ³¹,
 H. Lacker ¹⁷, D. Lacour ⁸², V.R. Lacuesta ¹⁶⁷, E. Ladygin ⁶⁷, R. Lafaye ⁵, B. Laforge ⁸², T. Lagouri ¹⁷⁶, S. Lai ⁵⁶,
 S. Lammers ⁶³, W. Lampl ⁷, E. Lançon ¹³⁷, U. Landgraf ⁵⁰, M.P.J. Landon ⁷⁸, V.S. Lang ^{60a}, J.C. Lange ¹³,
 A.J. Lankford ¹⁶³, F. Lanni ²⁷, K. Lantzsch ²³, A. Lanza ^{122a}, S. Laplace ⁸², C. Lapoire ³², J.F. Laporte ¹³⁷,
 T. Lari ^{93a}, F. Lasagni Manghi ^{22a,22b}, M. Lassnig ³², P. Laurelli ⁴⁹, W. Lavrijsen ¹⁶, A.T. Law ¹³⁸, P. Laycock ⁷⁶,
 T. Lazovich ⁵⁹, M. Lazzaroni ^{93a,93b}, B. Le ⁹⁰, O. Le Dortz ⁸², E. Le Guirriec ⁸⁷, E.P. Le Quilleuc ¹³⁷,
 M. LeBlanc ¹⁶⁹, T. LeCompte ⁶, F. Ledroit-Guillon ⁵⁷, C.A. Lee ²⁷, S.C. Lee ¹⁵², L. Lee ¹, G. Lefebvre ⁸²,
 M. Lefebvre ¹⁶⁹, F. Legger ¹⁰¹, C. Leggett ¹⁶, A. Lehan ⁷⁶, G. Lehmann Miotto ³², X. Lei ⁷, W.A. Leight ³¹,
 A. Leisos ^{155,ab}, A.G. Leister ¹⁷⁶, M.A.L. Leite ^{26d}, R. Leitner ¹³⁰, D. Lellouch ¹⁷², B. Lemmer ⁵⁶,
 K.J.C. Leney ⁸⁰, T. Lenz ²³, B. Lenzi ³², R. Leone ⁷, S. Leone ^{125a,125b}, C. Leonidopoulos ⁴⁸, S. Leontsinis ¹⁰,
 G. Lerner ¹⁵⁰, C. Leroy ⁹⁶, A.A.J. Lesage ¹³⁷, C.G. Lester ³⁰, M. Levchenko ¹²⁴, J. Levêque ⁵, D. Levin ⁹¹,
 L.J. Levinson ¹⁷², M. Levy ¹⁹, D. Lewis ⁷⁸, A.M. Leyko ²³, M. Leyton ⁴³, B. Li ^{35b,o}, H. Li ¹⁴⁹, H.L. Li ³³, L. Li ⁴⁷,
 L. Li ^{35e}, Q. Li ^{35a}, S. Li ⁴⁷, X. Li ⁸⁶, Y. Li ¹⁴², Z. Liang ^{35a}, B. Liberti ^{134a}, A. Liblong ¹⁵⁹, P. Lichard ³²,
 K. Lie ¹⁶⁶, J. Liebal ²³, W. Liebig ¹⁵, A. Limosani ¹⁵¹, S.C. Lin ^{152,ac}, T.H. Lin ⁸⁵, B.E. Lindquist ¹⁴⁹,
 A.E. Lioni ⁵¹, E. Lipeles ¹²³, A. Lipniacka ¹⁵, M. Lisovsky ^{60b}, T.M. Liss ¹⁶⁶, A. Lister ¹⁶⁸, A.M. Litke ¹³⁸,
 B. Liu ^{152,ad}, D. Liu ¹⁵², H. Liu ⁹¹, H. Liu ²⁷, J. Liu ⁸⁷, J.B. Liu ^{35b}, K. Liu ⁸⁷, L. Liu ¹⁶⁶, M. Liu ⁴⁷, M. Liu ^{35b},
 Y.L. Liu ^{35b}, Y. Liu ^{35b}, M. Livan ^{122a,122b}, A. Lleres ⁵⁷, J. Llorente Merino ^{35a}, S.L. Lloyd ⁷⁸, F. Lo Sterzo ¹⁵²,
 E. Lobodzinska ⁴⁴, P. Loch ⁷, W.S. Lockman ¹³⁸, F.K. Loebinger ⁸⁶, A.E. Loevschall-Jensen ³⁸, K.M. Loew ²⁵,
 A. Loginov ¹⁷⁶, T. Lohse ¹⁷, K. Lohwasser ⁴⁴, M. Lokajicek ¹²⁸, B.A. Long ²⁴, J.D. Long ¹⁶⁶, R.E. Long ⁷⁴,
 L. Longo ^{75a,75b}, K.A. Looper ¹¹², L. Lopes ^{127a}, D. Lopez Mateos ⁵⁹, B. Lopez Paredes ¹⁴⁰, I. Lopez Paz ¹³,
 A. Lopez Solis ⁸², J. Lorenz ¹⁰¹, N. Lorenzo Martinez ⁶³, M. Losada ²¹, P.J. Lösel ¹⁰¹, X. Lou ^{35a}, A. Lounis ¹¹⁸,
 J. Love ⁶, P.A. Love ⁷⁴, H. Lu ^{62a}, N. Lu ⁹¹, H.J. Lubatti ¹³⁹, C. Luci ^{133a,133b}, A. Lucotte ⁵⁷, C. Luedtke ⁵⁰,

F. Luehring⁶³, W. Lukas⁶⁴, L. Luminari^{133a}, O. Lundberg^{147a,147b}, B. Lund-Jensen¹⁴⁸, P.M. Luzi⁸², D. Lynn²⁷, R. Lysak¹²⁸, E. Lytken⁸³, V. Lyubushkin⁶⁷, H. Ma²⁷, L.L. Ma^{35d}, Y. Ma^{35d}, G. Maccarrone⁴⁹, A. Macchiolo¹⁰², C.M. Macdonald¹⁴⁰, B. Maček⁷⁷, J. Machado Miguens^{123,127b}, D. Madaffari⁸⁷, R. Madar³⁶, H.J. Maddocks¹⁶⁵, W.F. Mader⁴⁶, A. Madsen⁴⁴, J. Maeda⁶⁹, S. Maeland¹⁵, T. Maeno²⁷, A. Maeviskiy¹⁰⁰, E. Magradze⁵⁶, J. Mahlstedt¹⁰⁸, C. Maiani¹¹⁸, C. Maidantchik^{26a}, A.A. Maier¹⁰², T. Maier¹⁰¹, A. Maio^{127a,127b,127d}, S. Majewski¹¹⁷, Y. Makida⁶⁸, N. Makovec¹¹⁸, B. Malaescu⁸², Pa. Malecki⁴¹, V.P. Maleev¹²⁴, F. Malek⁵⁷, U. Mallik⁶⁵, D. Malon⁶, C. Malone¹⁴⁴, S. Maltezos¹⁰, S. Malyukov³², J. Mamuzic¹⁶⁷, G. Mancini⁴⁹, B. Mandelli³², L. Mandelli^{93a}, I. Mandić⁷⁷, J. Maneira^{127a,127b}, L. Manhaes de Andrade Filho^{26b}, J. Manjarres Ramos^{160b}, A. Mann¹⁰¹, A. Manousos³², B. Mansoulie¹³⁷, J.D. Mansour^{35a}, R. Mantifel⁸⁹, M. Mantoani⁵⁶, S. Manzoni^{93a,93b}, L. Mapelli³², G. Marceca²⁹, L. March⁵¹, G. Marchiori⁸², M. Marcisovsky¹²⁸, M. Marjanovic¹⁴, D.E. Marley⁹¹, F. Marroquim^{26a}, S.P. Marsden⁸⁶, Z. Marshall¹⁶, S. Marti-Garcia¹⁶⁷, B. Martin⁹², T.A. Martin¹⁷⁰, V.J. Martin⁴⁸, B. Martin dit Latour¹⁵, M. Martinez^{13,r}, V.I. Martinez Outschoorn¹⁶⁶, S. Martin-Haugh¹³², V.S. Martoiu^{28b}, A.C. Martyniuk⁸⁰, M. Marx¹³⁹, A. Marzin³², L. Masetti⁸⁵, T. Mashimo¹⁵⁶, R. Mashinistov⁹⁷, J. Masik⁸⁶, A.L. Maslennikov^{110,c}, I. Massa^{22a,22b}, L. Massa^{22a,22b}, P. Mastrandrea⁵, A. Mastroberardino^{39a,39b}, T. Masubuchi¹⁵⁶, P. Mättig¹⁷⁵, J. Mattmann⁸⁵, J. Maurer^{28b}, S.J. Maxfield⁷⁶, D.A. Maximov^{110,c}, R. Mazini¹⁵², S.M. Mazza^{93a,93b}, N.C. Mc Fadden¹⁰⁶, G. Mc Goldrick¹⁵⁹, S.P. Mc Kee⁹¹, A. McCarn⁹¹, R.L. McCarthy¹⁴⁹, T.G. McCarthy¹⁰², L.I. McClymont⁸⁰, E.F. McDonald⁹⁰, K.W. McFarlane^{58,*}, J.A. MCFayden⁸⁰, G. Mchedlidze⁵⁶, S.J. McMahon¹³², R.A. McPherson^{169,l}, M. Medinnis⁴⁴, S. Meehan¹³⁹, S. Mehlhase¹⁰¹, A. Mehta⁷⁶, K. Meier^{60a}, C. Meineck¹⁰¹, B. Meirose⁴³, D. Melini¹⁶⁷, B.R. Mellado Garcia^{146c}, M. Melo^{145a}, F. Meloni¹⁸, A. Mengarelli^{22a,22b}, S. Menke¹⁰², E. Meoni¹⁶², S. Mergelmeyer¹⁷, P. Mermoud⁵¹, L. Merola^{105a,105b}, C. Meroni^{93a}, F.S. Merritt³³, A. Messina^{133a,133b}, J. Metcalfe⁶, A.S. Mete¹⁶³, C. Meyer⁸⁵, C. Meyer¹²³, J.-P. Meyer¹³⁷, J. Meyer¹⁰⁸, H. Meyer Zu Theenhausen^{60a}, F. Miano¹⁵⁰, R.P. Middleton¹³², S. Miglioranza^{52a,52b}, L. Mijović²³, G. Mikenberg¹⁷², M. Mikestikova¹²⁸, M. Mikuž⁷⁷, M. Milesi⁹⁰, A. Milic⁶⁴, D.W. Miller³³, C. Mills⁴⁸, A. Milov¹⁷², D.A. Milstead^{147a,147b}, A.A. Minaenko¹³¹, Y. Minami¹⁵⁶, I.A. Minashvili⁶⁷, A.I. Mincer¹¹¹, B. Mindur^{40a}, M. Mineev⁶⁷, Y. Ming¹⁷³, L.M. Mir¹³, K.P. Mistry¹²³, T. Mitani¹⁷¹, J. Mitrevski¹⁰¹, V.A. Mitsou¹⁶⁷, A. Miucci⁵¹, P.S. Miyagawa¹⁴⁰, J.U. Mjörnmark⁸³, T. Moa^{147a,147b}, K. Mochizuki⁹⁶, S. Mohapatra³⁷, S. Molander^{147a,147b}, R. Moles-Valls²³, R. Monden⁷⁰, M.C. Mondragon⁹², K. Mönig⁴⁴, J. Monk³⁸, E. Monnier⁸⁷, A. Montalbano¹⁴⁹, J. Montejo Berlingen³², F. Monticelli⁷³, S. Monzani^{93a,93b}, R.W. Moore³, N. Morange¹¹⁸, D. Moreno²¹, M. Moreno Llácer⁵⁶, P. Morettini^{52a}, D. Mori¹⁴³, T. Mori¹⁵⁶, M. Morii⁵⁹, M. Morinaga¹⁵⁶, V. Morisbak¹²⁰, S. Moritz⁸⁵, A.K. Morley¹⁵¹, G. Mornacchi³², J.D. Morris⁷⁸, S.S. Mortensen³⁸, L. Morvaj¹⁴⁹, M. Mosidze^{53b}, J. Moss¹⁴⁴, K. Motohashi¹⁵⁸, R. Mount¹⁴⁴, E. Mountricha²⁷, S.V. Mouraviev^{97,*}, E.J.W. Moyse⁸⁸, S. Muanza⁸⁷, R.D. Mudd¹⁹, F. Mueller¹⁰², J. Mueller¹²⁶, R.S.P. Mueller¹⁰¹, T. Mueller³⁰, D. Muenstermann⁷⁴, P. Mullen⁵⁵, G.A. Mullier¹⁸, F.J. Munoz Sanchez⁸⁶, J.A. Murillo Quijada¹⁹, W.J. Murray^{170,132}, H. Musheghyan⁵⁶, M. Muškinja⁷⁷, A.G. Myagkov^{131,ae}, M. Myska¹²⁹, B.P. Nachman¹⁴⁴, O. Nackenhorst⁵¹, K. Nagai¹²¹, R. Nagai^{68,z}, K. Nagano⁶⁸, Y. Nagasaka⁶¹, K. Nagata¹⁶¹, M. Nagel⁵⁰, E. Nagy⁸⁷, A.M. Nairz³², Y. Nakahama³², K. Nakamura⁶⁸, T. Nakamura¹⁵⁶, I. Nakano¹¹³, H. Namasivayam⁴³, R.F. Naranjo Garcia⁴⁴, R. Narayan¹¹, D.I. Narrias Villar^{60a}, I. Naryshkin¹²⁴, T. Naumann⁴⁴, G. Navarro²¹, R. Nayyar⁷, H.A. Neal⁹¹, P.Yu. Nechaeva⁹⁷, T.J. Neep⁸⁶, P.D. Nef¹⁴⁴, A. Negri^{122a,122b}, M. Negrini^{22a}, S. Nektarijevic¹⁰⁷, C. Nellist¹¹⁸, A. Nelson¹⁶³, S. Nemecek¹²⁸, P. Nemethy¹¹¹, A.A. Nepomuceno^{26a}, M. Nessi^{32,af}, M.S. Neubauer¹⁶⁶, M. Neumann¹⁷⁵, R.M. Neves¹¹¹, P. Nevski²⁷, P.R. Newman¹⁹, D.H. Nguyen⁶, T. Nguyen Manh⁹⁶, R.B. Nickerson¹²¹, R. Nicolaidou¹³⁷, J. Nielsen¹³⁸, A. Nikiforov¹⁷, V. Nikolaenko^{131,ae}, I. Nikolic-Audit⁸², K. Nikolopoulos¹⁹, J.K. Nilsen¹²⁰, P. Nilsson²⁷, Y. Ninomiya¹⁵⁶, A. Nisati^{133a}, R. Nisius¹⁰², T. Nobe¹⁵⁶, L. Nodulman⁶, M. Nomachi¹¹⁹, I. Nomidis³¹, T. Nooney⁷⁸, S. Norberg¹¹⁴, M. Nordberg³², N. Norjoharuddeen¹²¹, O. Novgorodova⁴⁶, S. Nowak¹⁰², M. Nozaki⁶⁸, L. Nozka¹¹⁶, K. Ntekas¹⁰, E. Nurse⁸⁰, F. Nuti⁹⁰, F. O'grady⁷, D.C. O'Neil¹⁴³, A.A. O'Rourke⁴⁴, V. O'Shea⁵⁵, F.G. Oakham^{31,d}, H. Oberlack¹⁰², T. Obermann²³, J. Ocariz⁸², A. Ochi⁶⁹, I. Ochoa³⁷, J.P. Ochoa-Ricoux^{34a}, S. Oda⁷², S. Odaka⁶⁸, H. Ogren⁶³, A. Oh⁸⁶, S.H. Oh⁴⁷, C.C. Ohm¹⁶, H. Ohman¹⁶⁵, H. Oide³², H. Okawa¹⁶¹, Y. Okumura³³, T. Okuyama⁶⁸, A. Olariu^{28b}, L.F. Oleiro Seabra^{127a}, S.A. Olivares Pino⁴⁸,

D. Oliveira Damazio²⁷, A. Olszewski⁴¹, J. Olszowska⁴¹, A. Onofre^{127a,127e}, K. Onogi¹⁰⁴, P.U.E. Onyisi^{11,v}, M.J. Oreglia³³, Y. Oren¹⁵⁴, D. Orestano^{135a,135b}, N. Orlando^{62b}, R.S. Orr¹⁵⁹, B. Osculati^{52a,52b}, R. Ospanov⁸⁶, G. Otero y Garzon²⁹, H. Otono⁷², M. Ouchrif^{136d}, F. Ould-Saada¹²⁰, A. Ouraou¹³⁷, K.P. Oussoren¹⁰⁸, Q. Ouyang^{35a}, M. Owen⁵⁵, R.E. Owen¹⁹, V.E. Ozcan^{20a}, N. Ozturk⁸, K. Pachal¹⁴³, A. Pacheco Pages¹³, L. Pacheco Rodriguez¹³⁷, C. Padilla Aranda¹³, M. Pagáčová⁵⁰, S. Pagan Griso¹⁶, F. Paige²⁷, P. Pais⁸⁸, K. Pajchel¹²⁰, G. Palacino^{160b}, S. Palestini³², M. Palka^{40b}, D. Pallin³⁶, A. Palma^{127a,127b}, E.St. Panagiotopoulou¹⁰, C.E. Pandini⁸², J.G. Panduro Vazquez⁷⁹, P. Pani^{147a,147b}, S. Panitkin²⁷, D. Pantea^{28b}, L. Paolozzi⁵¹, Th.D. Papadopoulou¹⁰, K. Papageorgiou¹⁵⁵, A. Paramonov⁶, D. Paredes Hernandez¹⁷⁶, A.J. Parker⁷⁴, M.A. Parker³⁰, K.A. Parker¹⁴⁰, F. Parodi^{52a,52b}, J.A. Parsons³⁷, U. Parzefall⁵⁰, V.R. Pascuzzi¹⁵⁹, E. Pasqualucci^{133a}, S. Passaggio^{52a}, Fr. Pastore⁷⁹, G. Pásztor^{31,ag}, S. Patariaia¹⁷⁵, J.R. Pater⁸⁶, T. Pauly³², J. Pearce¹⁶⁹, B. Pearson¹¹⁴, L.E. Pedersen³⁸, M. Pedersen¹²⁰, S. Pedraza Lopez¹⁶⁷, R. Pedro^{127a,127b}, S.V. Peleganchuk^{110,c}, D. Pelikan¹⁶⁵, O. Penc¹²⁸, C. Peng^{35a}, H. Peng^{35b}, J. Penwell⁶³, B.S. Peralva^{26b}, M.M. Perego¹³⁷, D.V. Perepelitsa²⁷, E. Perez Codina^{160a}, L. Perini^{93a,93b}, H. Pernegger³², S. Perrella^{105a,105b}, R. Peschke⁴⁴, V.D. Peshekhonov⁶⁷, K. Peters⁴⁴, R.F.Y. Peters⁸⁶, B.A. Petersen³², T.C. Petersen³⁸, E. Petit⁵⁷, A. Petridis¹, C. Petridou¹⁵⁵, P. Petroff¹¹⁸, E. Petrolo^{133a}, M. Petrov¹²¹, F. Petrucci^{135a,135b}, N.E. Pettersson⁸⁸, A. Peyaud¹³⁷, R. Pezoa^{34b}, P.W. Phillips¹³², G. Piacquadio¹⁴⁴, E. Pianori¹⁷⁰, A. Picazio⁸⁸, E. Piccaro⁷⁸, M. Piccinini^{22a,22b}, M.A. Pickering¹²¹, R. Piegaia²⁹, J.E. Pilcher³³, A.D. Pilkington⁸⁶, A.W.J. Pin⁸⁶, M. Pinamonti^{164a,164c,ah}, J.L. Pinfold³, A. Pingel³⁸, S. Pires⁸², H. Pirumov⁴⁴, M. Pitt¹⁷², L. Plazak^{145a}, M.-A. Pleier²⁷, V. Pleskot⁸⁵, E. Plotnikova⁶⁷, P. Plucinski⁹², D. Pluth⁶⁶, R. Poettgen^{147a,147b}, L. Poggioli¹¹⁸, D. Pohl²³, G. Polesello^{122a}, A. Poley⁴⁴, A. Policicchio^{39a,39b}, R. Polifka¹⁵⁹, A. Polini^{22a}, C.S. Pollard⁵⁵, V. Polychronakos²⁷, K. Pommès³², L. Pontecorvo^{133a}, B.G. Pope⁹², G.A. Popeneciu^{28c}, D.S. Popovic¹⁴, A. Poppleton³², S. Pospisil¹²⁹, K. Potamianos¹⁶, I.N. Potrap⁶⁷, C.J. Potter³⁰, C.T. Potter¹¹⁷, G. Poulard³², J. Poveda³², V. Pozdnyakov⁶⁷, M.E. Pozo Astigarraga³², P. Pralavorio⁸⁷, A. Pranko¹⁶, S. Prell⁶⁶, D. Price⁸⁶, L.E. Price⁶, M. Primavera^{75a}, S. Prince⁸⁹, M. Proissl⁴⁸, K. Prokofiev^{62c}, F. Prokoshin^{34b}, S. Protopopescu²⁷, J. Proudfoot⁶, M. Przybycien^{40a}, D. Puddu^{135a,135b}, M. Purohit^{27,ai}, P. Puzo¹¹⁸, J. Qian⁹¹, G. Qin⁵⁵, Y. Qin⁸⁶, A. Quadt⁵⁶, W.B. Quayle^{164a,164b}, M. Queitsch-Maitland⁸⁶, D. Quilty⁵⁵, S. Raddum¹²⁰, V. Radeka²⁷, V. Radescu^{60b}, S.K. Radhakrishnan¹⁴⁹, P. Radloff¹¹⁷, P. Rados⁹⁰, F. Ragusa^{93a,93b}, G. Rahal¹⁷⁸, J.A. Raine⁸⁶, S. Rajagopalan²⁷, M. Rammensee³², C. Rangel-Smith¹⁶⁵, M.G. Ratti^{93a,93b}, F. Rauscher¹⁰¹, S. Rave⁸⁵, T. Ravenscroft⁵⁵, I. Ravinovich¹⁷², M. Raymond³², A.L. Read¹²⁰, N.P. Readioff⁷⁶, M. Reale^{75a,75b}, D.M. Rebutzi^{122a,122b}, A. Redelbach¹⁷⁴, G. Redlinger²⁷, R. Reece¹³⁸, K. Reeves⁴³, L. Rehnisch¹⁷, J. Reichert¹²³, H. Reisin²⁹, C. Rembser³², H. Ren^{35a}, M. Rescigno^{133a}, S. Resconi^{93a}, S. Rettie¹⁶⁸, O.L. Rezanova^{110,c}, P. Reznicek¹³⁰, R. Rezvani⁹⁶, R. Richter¹⁰², S. Richter⁸⁰, E. Richter-Was^{40b}, O. Ricken²³, M. Ridel⁸², P. Rieck¹⁷, C.J. Riegel¹⁷⁵, J. Rieger⁵⁶, O. Rifki¹¹⁴, M. Rijssenbeek¹⁴⁹, A. Rimoldi^{122a,122b}, M. Rimoldi¹⁸, L. Rinaldi^{22a}, B. Ristić⁵¹, E. Ritsch³², I. Riu¹³, F. Rizatdinova¹¹⁵, E. Rizvi⁷⁸, C. Rizzi¹³, S.H. Robertson^{89,l}, A. Robichaud-Veronneau⁸⁹, D. Robinson³⁰, J.E.M. Robinson⁴⁴, A. Robson⁵⁵, C. Roda^{125a,125b}, Y. Rodina⁸⁷, A. Rodriguez Perez¹³, D. Rodriguez Rodriguez¹⁶⁷, S. Roe³², C.S. Rogan⁵⁹, O. Röhne¹²⁰, A. Romaniouk⁹⁹, M. Romano^{22a,22b}, S.M. Romano Saez³⁶, E. Romero Adam¹⁶⁷, N. Rompotis¹³⁹, M. Ronzani⁵⁰, L. Roos⁸², E. Ros¹⁶⁷, S. Rosati^{133a}, K. Rosbach⁵⁰, P. Rose¹³⁸, O. Rosenthal¹⁴², N.-A. Rosien⁵⁶, V. Rossetti^{147a,147b}, E. Rossi^{105a,105b}, L.P. Rossi^{52a}, J.H.N. Rosten³⁰, R. Rosten¹³⁹, M. Rotaru^{28b}, I. Roth¹⁷², J. Rothberg¹³⁹, D. Rousseau¹¹⁸, C.R. Royon¹³⁷, A. Rozanov⁸⁷, Y. Rozen¹⁵³, X. Ruan^{146c}, F. Rubbo¹⁴⁴, M.S. Rudolph¹⁵⁹, F. Rühr⁵⁰, A. Ruiz-Martinez³¹, Z. Rurikova⁵⁰, N.A. Rusakovich⁶⁷, A. Ruschke¹⁰¹, H.L. Russell¹³⁹, J.P. Rutherford⁷, N. Ruthmann³², Y.F. Ryabov¹²⁴, M. Rybar¹⁶⁶, G. Rybkin¹¹⁸, S. Ryu⁶, A. Ryzhov¹³¹, G.F. Rzehorz⁵⁶, A.F. Saavedra¹⁵¹, G. Sabato¹⁰⁸, S. Sacerdoti²⁹, H.F.W. Sadrozinski¹³⁸, R. Sadykov⁶⁷, F. Safai Tehrani^{133a}, P. Saha¹⁰⁹, M. Sahinsoy^{60a}, M. Saimpert¹³⁷, T. Saito¹⁵⁶, H. Sakamoto¹⁵⁶, Y. Sakurai¹⁷¹, G. Salamanna^{135a,135b}, A. Salamon^{134a,134b}, J.E. Salazar Loyola^{34b}, D. Salek¹⁰⁸, P.H. Sales De Bruin¹³⁹, D. Salihagic¹⁰², A. Salnikov¹⁴⁴, J. Salt¹⁶⁷, D. Salvatore^{39a,39b}, F. Salvatore¹⁵⁰, A. Salvucci^{62a}, A. Salzburger³², D. Sammel⁵⁰, D. Sampsonidis¹⁵⁵, A. Sanchez^{105a,105b}, J. Sánchez¹⁶⁷, V. Sanchez Martinez¹⁶⁷, H. Sandaker¹²⁰, R.L. Sandbach⁷⁸, H.G. Sander⁸⁵, M. Sandhoff¹⁷⁵, C. Sandoval²¹, R. Sandstroem¹⁰², D.P.C. Sankey¹³², M. Sannino^{52a,52b}, A. Sansoni⁴⁹, C. Santoni³⁶, R. Santonico^{134a,134b}, H. Santos^{127a}, I. Santoyo Castillo¹⁵⁰, K. Sapp¹²⁶, A. Saprnov⁶⁷, J.G. Saraiva^{127a,127d}, B. Sarrazin²³,

O. Sasaki⁶⁸, Y. Sasaki¹⁵⁶, K. Sato¹⁶¹, G. Sauvage^{5,*}, E. Sauvan⁵, G. Savage⁷⁹, P. Savard^{159,d},
 C. Sawyer¹³², L. Sawyer^{81,q}, J. Saxon³³, C. Sbarra^{22a}, A. Sbrizzi^{22a,22b}, T. Scanlon⁸⁰, D.A. Scannicchio¹⁶³,
 M. Scarcella¹⁵¹, V. Scarfone^{39a,39b}, J. Schaarschmidt¹⁷², P. Schacht¹⁰², B.M. Schachtner¹⁰¹, D. Schaefer³²,
 R. Schaefer⁴⁴, J. Schaeffer⁸⁵, S. Schaepe²³, S. Schaetzel^{60b}, U. Schäfer⁸⁵, A.C. Schaffer¹¹⁸, D. Schaile¹⁰¹,
 R.D. Schamberger¹⁴⁹, V. Scharf^{60a}, V.A. Schegelsky¹²⁴, D. Scheirich¹³⁰, M. Schernau¹⁶³, C. Schiavi^{52a,52b},
 S. Schier¹³⁸, C. Schillo⁵⁰, M. Schioppa^{39a,39b}, S. Schlenker³², K.R. Schmidt-Sommerfeld¹⁰²,
 K. Schmieden³², C. Schmitt⁸⁵, S. Schmitt⁴⁴, S. Schmitz⁸⁵, B. Schneider^{160a}, U. Schnoor⁵⁰,
 L. Schoeffel¹³⁷, A. Schoening^{60b}, B.D. Schoenrock⁹², E. Schopf²³, M. Schott⁸⁵, J. Schovancova⁸,
 S. Schramm⁵¹, M. Schreyer¹⁷⁴, N. Schuh⁸⁵, A. Schulte⁸⁵, M.J. Schultens²³, H.-C. Schultz-Coulon^{60a},
 H. Schulz¹⁷, M. Schumacher⁵⁰, B.A. Schumm¹³⁸, Ph. Schune¹³⁷, A. Schwartzman¹⁴⁴, T.A. Schwarz⁹¹,
 Ph. Schwegler¹⁰², H. Schweiger⁸⁶, Ph. Schwemling¹³⁷, R. Schwienhorst⁹², J. Schwindling¹³⁷,
 T. Schwindt²³, G. Sciolla²⁵, F. Scuri^{125a,125b}, F. Scutti⁹⁰, J. Searcy⁹¹, P. Seema²³, S.C. Seidel¹⁰⁶,
 A. Seiden¹³⁸, F. Seifert¹²⁹, J.M. Seixas^{26a}, G. Sekhniaidze^{105a}, K. Sekhon⁹¹, S.J. Sekula⁴²,
 D.M. Seliverstov^{124,*}, N. Semprini-Cesari^{22a,22b}, C. Serfon¹²⁰, L. Serin¹¹⁸, L. Serkin^{164a,164b},
 M. Sessa^{135a,135b}, R. Seuster¹⁶⁹, H. Severini¹¹⁴, T. Sfiligoi⁷⁷, F. Sforza³², A. Sfyrla⁵¹, E. Shabalina⁵⁶,
 N.W. Shaikh^{147a,147b}, L.Y. Shan^{35a}, R. Shang¹⁶⁶, J.T. Shank²⁴, M. Shapiro¹⁶, P.B. Shatalov⁹⁸,
 K. Shaw^{164a,164b}, S.M. Shaw⁸⁶, A. Shcherbakova^{147a,147b}, C.Y. Shehu¹⁵⁰, P. Sherwood⁸⁰, L. Shi^{152,aj},
 S. Shimizu⁶⁹, C.O. Shimmin¹⁶³, M. Shimojima¹⁰³, M. Shiyakova^{67,ak}, A. Shmeleva⁹⁷, D. Shoaleh Saadi⁹⁶,
 M.J. Shochet³³, S. Shojaii^{93a,93b}, S. Shrestha¹¹², E. Shulga⁹⁹, M.A. Shupe⁷, P. Sicho¹²⁸, A.M. Sickles¹⁶⁶,
 P.E. Sidebo¹⁴⁸, O. Sidiropoulou¹⁷⁴, D. Sidorov¹¹⁵, A. Sidoti^{22a,22b}, F. Siegert⁴⁶, Dj. Sijacki¹⁴,
 J. Silva^{127a,127d}, S.B. Silverstein^{147a}, V. Simak¹²⁹, O. Simard⁵, Lj. Simic¹⁴, S. Simion¹¹⁸, E. Simioni⁸⁵,
 B. Simmons⁸⁰, D. Simon³⁶, M. Simon⁸⁵, P. Sinervo¹⁵⁹, N.B. Sinev¹¹⁷, M. Sioli^{22a,22b}, G. Siragusa¹⁷⁴,
 S.Yu. Sivoklokov¹⁰⁰, J. Sjölin^{147a,147b}, M.B. Skinner⁷⁴, H.P. Skottowe⁵⁹, P. Skubic¹¹⁴, M. Slater¹⁹,
 T. Slavicek¹²⁹, M. Slawinska¹⁰⁸, K. Sliwa¹⁶², R. Slovak¹³⁰, V. Smakhtin¹⁷², B.H. Smart⁵, L. Smestad¹⁵,
 J. Smiesko^{145a}, S.Yu. Smirnov⁹⁹, Y. Smirnov⁹⁹, L.N. Smirnova^{100,al}, O. Smirnova⁸³, M.N.K. Smith³⁷,
 R.W. Smith³⁷, M. Smizanska⁷⁴, K. Smolek¹²⁹, A.A. Snesarev⁹⁷, S. Snyder²⁷, R. Sobie^{169,l}, F. Socher⁴⁶,
 A. Soffer¹⁵⁴, D.A. Soh¹⁵², G. Sokhrannyi⁷⁷, C.A. Solans Sanchez³², M. Solar¹²⁹, E.Yu. Soldatov⁹⁹,
 U. Soldevila¹⁶⁷, A.A. Solodkov¹³¹, A. Soloshenko⁶⁷, O.V. Solovyanov¹³¹, V. Solovyev¹²⁴, P. Sommer⁵⁰,
 H. Son¹⁶², H.Y. Song^{35b,am}, A. Sood¹⁶, A. Sopczak¹²⁹, V. Sopko¹²⁹, V. Sorin¹³, D. Sosa^{60b},
 C.L. Sotiropoulou^{125a,125b}, R. Soualah^{164a,164c}, A.M. Soukharev^{110,c}, D. South⁴⁴, B.C. Sowden⁷⁹,
 S. Spagnolo^{75a,75b}, M. Spalla^{125a,125b}, M. Spangenberg¹⁷⁰, F. Spanò⁷⁹, D. Sperlich¹⁷, F. Spettel¹⁰²,
 R. Spighi^{22a}, G. Spigo³², L.A. Spiller⁹⁰, M. Spousta¹³⁰, R.D. St. Denis^{55,*}, A. Stabile^{93a}, R. Stamen^{60a},
 S. Stamm¹⁷, E. Stanecka⁴¹, R.W. Stanek⁶, C. Stanescu^{135a}, M. Stanescu-Bellu⁴⁴, M.M. Stanitzki⁴⁴,
 S. Stapnes¹²⁰, E.A. Starchenko¹³¹, G.H. Stark³³, J. Stark⁵⁷, P. Staroba¹²⁸, P. Starovoitov^{60a}, S. Stärz³²,
 R. Staszewski⁴¹, P. Steinberg²⁷, B. Stelzer¹⁴³, H.J. Stelzer³², O. Stelzer-Chilton^{160a}, H. Stenzel⁵⁴,
 G.A. Stewart⁵⁵, J.A. Stillings²³, M.C. Stockton⁸⁹, M. Stoebe⁸⁹, G. Stoicea^{28b}, P. Stolte⁵⁶, S. Stonjek¹⁰²,
 A.R. Stradling⁸, A. Straessner⁴⁶, M.E. Stramaglia¹⁸, J. Strandberg¹⁴⁸, S. Strandberg^{147a,147b},
 A. Strandlie¹²⁰, M. Strauss¹¹⁴, P. Strizenec^{145b}, R. Ströhmer¹⁷⁴, D.M. Strom¹¹⁷, R. Stroynowski⁴²,
 A. Strubig¹⁰⁷, S.A. Stucci¹⁸, B. Stugu¹⁵, N.A. Styles⁴⁴, D. Su¹⁴⁴, J. Su¹²⁶, R. Subramaniam⁸¹,
 S. Suchek^{60a}, Y. Sugaya¹¹⁹, M. Suk¹²⁹, V.V. Sulin⁹⁷, S. Sultansoy^{4c}, T. Sumida⁷⁰, S. Sun⁵⁹, X. Sun^{35a},
 J.E. Sundermann⁵⁰, K. Suruliz¹⁵⁰, G. Susinno^{39a,39b}, M.R. Sutton¹⁵⁰, S. Suzuki⁶⁸, M. Svatos¹²⁸,
 M. Swiatlowski³³, I. Sykora^{145a}, T. Sykora¹³⁰, D. Ta⁵⁰, C. Taccini^{135a,135b}, K. Tackmann⁴⁴, J. Taenzer¹⁵⁹,
 A. Taffard¹⁶³, R. Tahirout^{160a}, N. Taiblum¹⁵⁴, H. Takai²⁷, R. Takashima⁷¹, T. Takeshita¹⁴¹, Y. Takubo⁶⁸,
 M. Talby⁸⁷, A.A. Talyshev^{110,c}, K.G. Tan⁹⁰, J. Tanaka¹⁵⁶, R. Tanaka¹¹⁸, S. Tanaka⁶⁸, B.B. Tannenwald¹¹²,
 S. Tapia Araya^{34b}, S. Tapprogge⁸⁵, S. Tarem¹⁵³, G.F. Tartarelli^{93a}, P. Tas¹³⁰, M. Tasevsky¹²⁸, T. Tashiro⁷⁰,
 E. Tassi^{39a,39b}, A. Tavares Delgado^{127a,127b}, Y. Tayalati^{136d}, A.C. Taylor¹⁰⁶, G.N. Taylor⁹⁰, P.T.E. Taylor⁹⁰,
 W. Taylor^{160b}, F.A. Teischinger³², P. Teixeira-Dias⁷⁹, K.K. Temming⁵⁰, D. Temple¹⁴³, H. Ten Kate³²,
 P.K. Teng¹⁵², J.J. Teoh¹¹⁹, F. Tepel¹⁷⁵, S. Terada⁶⁸, K. Terashi¹⁵⁶, J. Terron⁸⁴, S. Terzo¹⁰², M. Testa⁴⁹,
 R.J. Teuscher^{159,l}, T. Thevenaux-Pelzer⁸⁷, J.P. Thomas¹⁹, J. Thomas-Wilsker⁷⁹, E.N. Thompson³⁷,
 P.D. Thompson¹⁹, A.S. Thompson⁵⁵, L.A. Thomsen¹⁷⁶, E. Thomson¹²³, M. Thomson³⁰, M.J. Tibbetts¹⁶,
 R.E. Ticse Torres⁸⁷, V.O. Tikhomirov^{97,an}, Yu.A. Tikhonov^{110,c}, S. Timoshenko⁹⁹, P. Tipton¹⁷⁶,
 S. Tisserant⁸⁷, K. Todome¹⁵⁸, T. Todorov^{5,*}, S. Todorova-Nova¹³⁰, J. Tojo⁷², S. Tokár^{145a},

K. Tokushuku⁶⁸, E. Tolley⁵⁹, L. Tomlinson⁸⁶, M. Tomoto¹⁰⁴, L. Tompkins^{144,ao}, K. Toms¹⁰⁶, B. Tong⁵⁹,
 E. Torrence¹¹⁷, H. Torres¹⁴³, E. Torró Pastor¹³⁹, J. Toth^{87,ap}, F. Touchard⁸⁷, D.R. Tovey¹⁴⁰, T. Trefzger¹⁷⁴,
 A. Tricoli²⁷, I.M. Trigger^{160a}, S. Trincaz-Duvoid⁸², M.F. Tripiana¹³, W. Trischuk¹⁵⁹, B. Trocmé⁵⁷,
 A. Trofymov⁴⁴, C. Troncon^{93a}, M. Trottier-McDonald¹⁶, M. Trovatelli¹⁶⁹, L. Truong^{164a,164c},
 M. Trzebinski⁴¹, A. Trzupek⁴¹, J.C.-L. Tseng¹²¹, P.V. Tsiareshka⁹⁴, G. Tsipolitis¹⁰, N. Tsirintanis⁹,
 S. Tsiskaridze¹³, V. Tsiskaridze⁵⁰, E.G. Tskhadadze^{53a}, K.M. Tsui^{62a}, I.I. Tsukerman⁹⁸, V. Tsulaia¹⁶,
 S. Tsuno⁶⁸, D. Tsybychev¹⁴⁹, A. Tudorache^{28b}, V. Tudorache^{28b}, A.N. Tuna⁵⁹, S.A. Tuppuri^{22a,22b},
 S. Turchikhin^{100,al}, D. Turecek¹²⁹, D. Turgeman¹⁷², R. Turra^{93a,93b}, A.J. Turvey⁴², P.M. Tuts³⁷,
 M. Tyndel¹³², G. Ucchielli^{22a,22b}, I. Ueda¹⁵⁶, M. Ughetto^{147a,147b}, F. Ukegawa¹⁶¹, G. Unal³²,
 A. Undrus²⁷, G. Unel¹⁶³, F.C. Ungaro⁹⁰, Y. Unno⁶⁸, C. Unverdorben¹⁰¹, J. Urban^{145b}, P. Urquijo⁹⁰,
 P. Urrejola⁸⁵, G. Usai⁸, A. Usanova⁶⁴, L. Vacavant⁸⁷, V. Vacek¹²⁹, B. Vachon⁸⁹, C. Valderanis¹⁰¹,
 E. Valdes Santurio^{147a,147b}, N. Valencic¹⁰⁸, S. Valentineti^{22a,22b}, A. Valero¹⁶⁷, L. Valery¹³, S. Valkar¹³⁰,
 S. Vallecorsa⁵¹, J.A. Valls Ferrer¹⁶⁷, W. Van Den Wollenberg¹⁰⁸, P.C. Van Der Deijl¹⁰⁸,
 R. van der Geer¹⁰⁸, H. van der Graaf¹⁰⁸, N. van Eldik¹⁵³, P. van Gemmeren⁶, J. Van Nieuwkoop¹⁴³,
 I. van Vulpen¹⁰⁸, M.C. van Woerden³², M. Vanadia^{133a,133b}, W. Vandelli³², R. Vanguri¹²³,
 A. Vaniachine¹³¹, P. Vankov¹⁰⁸, G. Vardanyan¹⁷⁷, R. Vari^{133a}, E.W. Varnes⁷, T. Varol⁴², D. Varouchas⁸²,
 A. Vartapetian⁸, K.E. Varvell¹⁵¹, J.G. Vasquez¹⁷⁶, F. Vazeille³⁶, T. Vazquez Schroeder⁸⁹, J. Veatch⁵⁶,
 L.M. Veloce¹⁵⁹, F. Veloso^{127a,127c}, S. Veneziano^{133a}, A. Ventura^{75a,75b}, M. Venturi¹⁶⁹, N. Venturi¹⁵⁹,
 A. Venturini²⁵, V. Vercesi^{122a}, M. Verducci^{133a,133b}, W. Verkerke¹⁰⁸, J.C. Vermeulen¹⁰⁸, A. Vest^{46,aq},
 M.C. Vetterli^{143,d}, O. Viazlo⁸³, I. Vichou¹⁶⁶, T. Vickey¹⁴⁰, O.E. Vickey Boeriu¹⁴⁰, G.H.A. Viehhauser¹²¹,
 S. Viel¹⁶, L. Vigani¹²¹, R. Vigne⁶⁴, M. Villa^{22a,22b}, M. Villaplana Perez^{93a,93b}, E. Vilucchi⁴⁹,
 M.G. Vincter³¹, V.B. Vinogradov⁶⁷, C. Vittori^{22a,22b}, I. Vivarelli¹⁵⁰, S. Vlachos¹⁰, M. Vlasak¹²⁹,
 M. Vogel¹⁷⁵, P. Vokac¹²⁹, G. Volpi^{125a,125b}, M. Volpi⁹⁰, H. von der Schmitt¹⁰², E. von Toerne²³,
 V. Vorobel¹³⁰, K. Vorobev⁹⁹, M. Vos¹⁶⁷, R. Voss³², J.H. Vossebeld⁷⁶, N. Vranjes¹⁴,
 M. Vranjes Milosavljevic¹⁴, V. Vrba¹²⁸, M. Vreeswijk¹⁰⁸, R. Vuillermet³², I. Vukotic³³, Z. Vykydal¹²⁹,
 P. Wagner²³, W. Wagner¹⁷⁵, H. Wahlberg⁷³, S. Wahrmund⁴⁶, J. Wakabayashi¹⁰⁴, J. Walder⁷⁴,
 R. Walker¹⁰¹, W. Walkowiak¹⁴², V. Wallangen^{147a,147b}, C. Wang^{35c}, C. Wang^{35d,87}, F. Wang¹⁷³,
 H. Wang¹⁶, H. Wang⁴², J. Wang⁴⁴, J. Wang¹⁵¹, K. Wang⁸⁹, R. Wang⁶, S.M. Wang¹⁵², T. Wang²³,
 T. Wang³⁷, W. Wang^{35b}, X. Wang¹⁷⁶, C. Wanotayaroj¹¹⁷, A. Warburton⁸⁹, C.P. Ward³⁰, D.R. Wardrope⁸⁰,
 A. Washbrook⁴⁸, P.M. Watkins¹⁹, A.T. Watson¹⁹, M.F. Watson¹⁹, G. Watts¹³⁹, S. Watts⁸⁶, B.M. Waugh⁸⁰,
 S. Webb⁸⁵, M.S. Weber¹⁸, S.W. Weber¹⁷⁴, J.S. Webster⁶, A.R. Weidberg¹²¹, B. Weinert⁶³,
 J. Weingarten⁵⁶, C. Weiser⁵⁰, H. Weits¹⁰⁸, P.S. Wells³², T. Wenaus²⁷, T. Wengler³², S. Wenig³²,
 N. Wermes²³, M. Werner⁵⁰, M.D. Werner⁶⁶, P. Werner³², M. Wessels^{60a}, J. Wetter¹⁶², K. Whalen¹¹⁷,
 N.L. Whallon¹³⁹, A.M. Wharton⁷⁴, A. White⁸, M.J. White¹, R. White^{34b}, D. Whiteson¹⁶³, F.J. Wickens¹³²,
 W. Wiedenmann¹⁷³, M. Wielers¹³², P. Wienemann²³, C. Wigglesworth³⁸, L.A.M. Wiik-Fuchs²³,
 A. Wildauer¹⁰², F. Wilk⁸⁶, H.G. Wilkens³², H.H. Williams¹²³, S. Williams¹⁰⁸, C. Willis⁹², S. Willocq⁸⁸,
 J.A. Wilson¹⁹, I. Wingerter-Seez⁵, F. Winklmeier¹¹⁷, O.J. Winston¹⁵⁰, B.T. Winter²³, M. Wittgen¹⁴⁴,
 J. Wittkowski¹⁰¹, M.W. Wolter⁴¹, H. Wolters^{127a,127c}, S.D. Worm¹³², B.K. Wosiek⁴¹, J. Wotschack³²,
 M.J. Woudstra⁸⁶, K.W. Wozniak⁴¹, M. Wu⁵⁷, M. Wu³³, S.L. Wu¹⁷³, X. Wu⁵¹, Y. Wu⁹¹, T.R. Wyatt⁸⁶,
 B.M. Wynne⁴⁸, S. Xella³⁸, D. Xu^{35a}, L. Xu²⁷, B. Yabsley¹⁵¹, S. Yacoob^{146a}, R. Yakabe⁶⁹, D. Yamaguchi¹⁵⁸,
 Y. Yamaguchi¹¹⁹, A. Yamamoto⁶⁸, S. Yamamoto¹⁵⁶, T. Yamanaka¹⁵⁶, K. Yamauchi¹⁰⁴, Y. Yamazaki⁶⁹,
 Z. Yan²⁴, H. Yang^{35e}, H. Yang¹⁷³, Y. Yang¹⁵², Z. Yang¹⁵, W.-M. Yao¹⁶, Y.C. Yap⁸², Y. Yasu⁶⁸, E. Yatsenko⁵,
 K.H. Yau Wong²³, J. Ye⁴², S. Ye²⁷, I. Yeletsikh⁶⁷, A.L. Yen⁵⁹, E. Yildirim⁸⁵, K. Yorita¹⁷¹, R. Yoshida⁶,
 K. Yoshihara¹²³, C. Young¹⁴⁴, C.J.S. Young³², S. Youssef²⁴, D.R. Yu¹⁶, J. Yu⁸, J.M. Yu⁹¹, J. Yu⁶⁶, L. Yuan⁶⁹,
 S.P.Y. Yuen²³, I. Yusuff^{30,ar}, B. Zabinski⁴¹, R. Zaidan^{35d}, A.M. Zaitsev^{131,ae}, N. Zakharchuk⁴⁴,
 J. Zalieckas¹⁵, A. Zaman¹⁴⁹, S. Zambito⁵⁹, L. Zanello^{133a,133b}, D. Zanzi⁹⁰, C. Zeitnitz¹⁷⁵, M. Zeman¹²⁹,
 A. Zemla^{40a}, J.C. Zeng¹⁶⁶, Q. Zeng¹⁴⁴, K. Zengel²⁵, O. Zenin¹³¹, T. Ženiš^{145a}, D. Zerwas¹¹⁸, D. Zhang⁹¹,
 F. Zhang¹⁷³, G. Zhang^{35b,am}, H. Zhang^{35c}, J. Zhang⁶, L. Zhang⁵⁰, R. Zhang²³, R. Zhang^{35b,as},
 X. Zhang^{35d}, Z. Zhang¹¹⁸, X. Zhao⁴², Y. Zhao^{35d}, Z. Zhao^{35b}, A. Zhemchugov⁶⁷, J. Zhong¹²¹, B. Zhou⁹¹,
 C. Zhou⁴⁷, L. Zhou³⁷, L. Zhou⁴², M. Zhou¹⁴⁹, N. Zhou^{35f}, C.G. Zhu^{35d}, H. Zhu^{35a}, J. Zhu⁹¹, Y. Zhu^{35b},
 X. Zhuang^{35a}, K. Zhukov⁹⁷, A. Zibell¹⁷⁴, D. Ziemska⁶³, N.I. Zimine⁶⁷, C. Zimmermann⁸⁵,

S. Zimmermann⁵⁰, Z. Zinonos⁵⁶, M. Zinser⁸⁵, M. Ziolkowski¹⁴², L. Živković¹⁴, G. Zobernig¹⁷³,
A. Zoccoli^{22a,22b}, M. zur Nedden¹⁷, L. Zwalinski³²

- ¹ Department of Physics, University of Adelaide, Adelaide, Australia
- ² Physics Department, SUNY Albany, Albany NY, United States
- ³ Department of Physics, University of Alberta, Edmonton AB, Canada
- ⁴ (a) Department of Physics, Ankara University, Ankara; (b) Istanbul Aydin University, Istanbul; (c) Division of Physics, TOBB University of Economics and Technology, Ankara, Turkey
- ⁵ LAPP, CNRS/IN2P3 and Université Savoie Mont Blanc, Annecy-le-Vieux, France
- ⁶ High Energy Physics Division, Argonne National Laboratory, Argonne IL, United States
- ⁷ Department of Physics, University of Arizona, Tucson AZ, United States
- ⁸ Department of Physics, The University of Texas at Arlington, Arlington TX, United States
- ⁹ Physics Department, University of Athens, Athens, Greece
- ¹⁰ Physics Department, National Technical University of Athens, Zografou, Greece
- ¹¹ Department of Physics, The University of Texas at Austin, Austin TX, United States
- ¹² Institute of Physics, Azerbaijan Academy of Sciences, Baku, Azerbaijan
- ¹³ Institut de Física d'Altes Energies (IFAE), The Barcelona Institute of Science and Technology, Barcelona, Spain
- ¹⁴ Institute of Physics, University of Belgrade, Belgrade, Serbia
- ¹⁵ Department for Physics and Technology, University of Bergen, Bergen, Norway
- ¹⁶ Physics Division, Lawrence Berkeley National Laboratory and University of California, Berkeley CA, United States
- ¹⁷ Department of Physics, Humboldt University, Berlin, Germany
- ¹⁸ Albert Einstein Center for Fundamental Physics and Laboratory for High Energy Physics, University of Bern, Bern, Switzerland
- ¹⁹ School of Physics and Astronomy, University of Birmingham, Birmingham, United Kingdom
- ²⁰ (a) Department of Physics, Bogazici University, Istanbul; (b) Department of Physics Engineering, Gaziantep University, Gaziantep; (d) Istanbul Bilgi University, Faculty of Engineering and Natural Sciences, Istanbul, Turkey; (e) Bahcesehir University, Faculty of Engineering and Natural Sciences, Istanbul, Turkey
- ²¹ Centro de Investigaciones, Universidad Antonio Narino, Bogota, Colombia
- ²² (a) INFN Sezione di Bologna; (b) Dipartimento di Fisica e Astronomia, Università di Bologna, Bologna, Italy
- ²³ Physikalisches Institut, University of Bonn, Bonn, Germany
- ²⁴ Department of Physics, Boston University, Boston MA, United States
- ²⁵ Department of Physics, Brandeis University, Waltham MA, United States
- ²⁶ (a) Universidade Federal do Rio De Janeiro COPPE/EE/IF, Rio de Janeiro; (b) Electrical Circuits Department, Federal University of Juiz de Fora (UFJF), Juiz de Fora; (c) Federal University of Sao Joao del Rei (UFSJ), Sao Joao del Rei; (d) Instituto de Fisica, Universidade de Sao Paulo, Sao Paulo, Brazil
- ²⁷ Physics Department, Brookhaven National Laboratory, Upton NY, United States
- ²⁸ (a) Transilvania University of Brasov, Brasov, Romania; (b) National Institute of Physics and Nuclear Engineering, Bucharest; (c) National Institute for Research and Development of Isotopic and Molecular Technologies, Physics Department, Cluj Napoca; (d) University Politehnica Bucharest, Bucharest; (e) West University in Timisoara, Timisoara, Romania
- ²⁹ Departamento de Física, Universidad de Buenos Aires, Buenos Aires, Argentina
- ³⁰ Cavendish Laboratory, University of Cambridge, Cambridge, United Kingdom
- ³¹ Department of Physics, Carleton University, Ottawa ON, Canada
- ³² CERN, Geneva, Switzerland
- ³³ Enrico Fermi Institute, University of Chicago, Chicago IL, United States
- ³⁴ (a) Departamento de Física, Pontificia Universidad Católica de Chile, Santiago; (b) Departamento de Física, Universidad Técnica Federico Santa María, Valparaíso, Chile
- ³⁵ (a) Institute of High Energy Physics, Chinese Academy of Sciences, Beijing; (b) Department of Modern Physics, University of Science and Technology of China, Anhui; (c) Department of Physics, Nanjing University, Jiangsu; (d) School of Physics, Shandong University, Shandong; (e) Department of Physics and Astronomy, Shanghai Key Laboratory for Particle Physics and Cosmology, Shanghai Jiao Tong University, Shanghai; (f) Physics Department, Tsinghua University, Beijing 100084, China
- ³⁶ Laboratoire de Physique Corpusculaire, Clermont Université and Université Blaise Pascal and CNRS/IN2P3, Clermont-Ferrand, France
- ³⁷ Nevis Laboratory, Columbia University, Irvington NY, United States
- ³⁸ Niels Bohr Institute, University of Copenhagen, Copenhagen, Denmark
- ³⁹ (a) INFN Gruppo Collegato di Cosenza, Laboratori Nazionali di Frascati; (b) Dipartimento di Fisica, Università della Calabria, Rende, Italy
- ⁴⁰ (a) AGH University of Science and Technology, Faculty of Physics and Applied Computer Science, Krakow; (b) Marian Smoluchowski Institute of Physics, Jagiellonian University, Krakow, Poland
- ⁴¹ Institute of Nuclear Physics Polish Academy of Sciences, Krakow, Poland
- ⁴² Physics Department, Southern Methodist University, Dallas TX, United States
- ⁴³ Physics Department, University of Texas at Dallas, Richardson TX, United States
- ⁴⁴ DESY, Hamburg and Zeuthen, Germany
- ⁴⁵ Institut für Experimentelle Physik IV, Technische Universität Dortmund, Dortmund, Germany
- ⁴⁶ Institut für Kern- und Teilchenphysik, Technische Universität Dresden, Dresden, Germany
- ⁴⁷ Department of Physics, Duke University, Durham NC, United States
- ⁴⁸ SUPA – School of Physics and Astronomy, University of Edinburgh, Edinburgh, United Kingdom
- ⁴⁹ INFN Laboratori Nazionali di Frascati, Frascati, Italy
- ⁵⁰ Fakultät für Mathematik und Physik, Albert-Ludwigs-Universität, Freiburg, Germany
- ⁵¹ Section de Physique, Université de Genève, Geneva, Switzerland
- ⁵² (a) INFN Sezione di Genova; (b) Dipartimento di Fisica, Università di Genova, Genova, Italy
- ⁵³ (a) E. Andronikashvili Institute of Physics, Iv. Javakishvili Tbilisi State University, Tbilisi; (b) High Energy Physics Institute, Tbilisi State University, Tbilisi, Georgia
- ⁵⁴ II Physikalisches Institut, Justus-Liebig-Universität Giessen, Giessen, Germany
- ⁵⁵ SUPA – School of Physics and Astronomy, University of Glasgow, Glasgow, United Kingdom
- ⁵⁶ II Physikalisches Institut, Georg-August-Universität, Göttingen, Germany
- ⁵⁷ Laboratoire de Physique Subatomique et de Cosmologie, Université Grenoble-Alpes, CNRS/IN2P3, Grenoble, France
- ⁵⁸ Department of Physics, Hampton University, Hampton VA, United States
- ⁵⁹ Laboratory for Particle Physics and Cosmology, Harvard University, Cambridge MA, United States
- ⁶⁰ (a) Kirchhoff-Institut für Physik, Ruprecht-Karls-Universität Heidelberg, Heidelberg; (b) Physikalisches Institut, Ruprecht-Karls-Universität Heidelberg, Mannheim, Germany
- ⁶¹ Faculty of Applied Information Science, Hiroshima Institute of Technology, Hiroshima, Japan
- ⁶² (a) Department of Physics, The Chinese University of Hong Kong, Shatin, N.T., Hong Kong; (b) Department of Physics, The University of Hong Kong, Hong Kong; (c) Department of Physics, The Hong Kong University of Science and Technology, Clear Water Bay, Kowloon, Hong Kong, China
- ⁶³ Department of Physics, Indiana University, Bloomington IN, United States
- ⁶⁴ Institut für Astro- und Teilchenphysik, Leopold-Franzens-Universität, Innsbruck, Austria
- ⁶⁵ University of Iowa, Iowa City IA, United States
- ⁶⁶ Department of Physics and Astronomy, Iowa State University, Ames IA, United States
- ⁶⁷ Joint Institute for Nuclear Research, JINR Dubna, Dubna, Russia

- ⁶⁸ KEK, High Energy Accelerator Research Organization, Tsukuba, Japan
- ⁶⁹ Graduate School of Science, Kobe University, Kobe, Japan
- ⁷⁰ Faculty of Science, Kyoto University, Kyoto, Japan
- ⁷¹ Kyoto University of Education, Kyoto, Japan
- ⁷² Department of Physics, Kyushu University, Fukuoka, Japan
- ⁷³ Instituto de Física La Plata, Universidad Nacional de La Plata and CONICET, La Plata, Argentina
- ⁷⁴ Physics Department, Lancaster University, Lancaster, United Kingdom
- ⁷⁵ ^(a) INFN Sezione di Lecce; ^(b) Dipartimento di Matematica e Fisica, Università del Salento, Lecce, Italy
- ⁷⁶ Oliver Lodge Laboratory, University of Liverpool, Liverpool, United Kingdom
- ⁷⁷ Department of Physics, Jožef Stefan Institute and University of Ljubljana, Ljubljana, Slovenia
- ⁷⁸ School of Physics and Astronomy, Queen Mary University of London, London, United Kingdom
- ⁷⁹ Department of Physics, Royal Holloway University of London, Surrey, United Kingdom
- ⁸⁰ Department of Physics and Astronomy, University College London, London, United Kingdom
- ⁸¹ Louisiana Tech University, Ruston LA, United States
- ⁸² Laboratoire de Physique Nucléaire et de Hautes Energies, UPMC and Université Paris-Diderot and CNRS/IN2P3, Paris, France
- ⁸³ Fysiska institutionen, Lunds universitet, Lund, Sweden
- ⁸⁴ Departamento de Física Teórica C-15, Universidad Autónoma de Madrid, Madrid, Spain
- ⁸⁵ Institut für Physik, Universität Mainz, Mainz, Germany
- ⁸⁶ School of Physics and Astronomy, University of Manchester, Manchester, United Kingdom
- ⁸⁷ CPPM, Aix-Marseille Université and CNRS/IN2P3, Marseille, France
- ⁸⁸ Department of Physics, University of Massachusetts, Amherst MA, United States
- ⁸⁹ Department of Physics, McGill University, Montreal QC, Canada
- ⁹⁰ School of Physics, University of Melbourne, Victoria, Australia
- ⁹¹ Department of Physics, The University of Michigan, Ann Arbor MI, United States
- ⁹² Department of Physics and Astronomy, Michigan State University, East Lansing MI, United States
- ⁹³ ^(a) INFN Sezione di Milano; ^(b) Dipartimento di Fisica, Università di Milano, Milano, Italy
- ⁹⁴ B.I. Stepanov Institute of Physics, National Academy of Sciences of Belarus, Minsk, Belarus
- ⁹⁵ National Scientific and Educational Centre for Particle and High Energy Physics, Minsk, Belarus
- ⁹⁶ Group of Particle Physics, University of Montreal, Montreal QC, Canada
- ⁹⁷ P.N. Lebedev Physical Institute of the Russian Academy of Sciences, Moscow, Russia
- ⁹⁸ Institute for Theoretical and Experimental Physics (ITEP), Moscow, Russia
- ⁹⁹ National Research Nuclear University MEPhI, Moscow, Russia
- ¹⁰⁰ D.V. Skobeltsyn Institute of Nuclear Physics, M.V. Lomonosov Moscow State University, Moscow, Russia
- ¹⁰¹ Fakultät für Physik, Ludwig-Maximilians-Universität München, München, Germany
- ¹⁰² Max-Planck-Institut für Physik (Werner-Heisenberg-Institut), München, Germany
- ¹⁰³ Nagasaki Institute of Applied Science, Nagasaki, Japan
- ¹⁰⁴ Graduate School of Science and Kobayashi-Maskawa Institute, Nagoya University, Nagoya, Japan
- ¹⁰⁵ ^(a) INFN Sezione di Napoli; ^(b) Dipartimento di Fisica, Università di Napoli, Napoli, Italy
- ¹⁰⁶ Department of Physics and Astronomy, University of New Mexico, Albuquerque NM, United States
- ¹⁰⁷ Institute for Mathematics, Astrophysics and Particle Physics, Radboud University Nijmegen/Nikhef, Nijmegen, Netherlands
- ¹⁰⁸ Nikhef National Institute for Subatomic Physics and University of Amsterdam, Amsterdam, Netherlands
- ¹⁰⁹ Department of Physics, Northern Illinois University, DeKalb IL, United States
- ¹¹⁰ Budker Institute of Nuclear Physics, SB RAS, Novosibirsk, Russia
- ¹¹¹ Department of Physics, New York University, New York NY, United States
- ¹¹² Ohio State University, Columbus OH, United States
- ¹¹³ Faculty of Science, Okayama University, Okayama, Japan
- ¹¹⁴ Homer L. Dodge Department of Physics and Astronomy, University of Oklahoma, Norman OK, United States
- ¹¹⁵ Department of Physics, Oklahoma State University, Stillwater OK, United States
- ¹¹⁶ Palacký University, RCPTM, Olomouc, Czech Republic
- ¹¹⁷ Center for High Energy Physics, University of Oregon, Eugene OR, United States
- ¹¹⁸ LAL, Univ. Paris-Sud, CNRS/IN2P3, Université Paris-Saclay, Orsay, France
- ¹¹⁹ Graduate School of Science, Osaka University, Osaka, Japan
- ¹²⁰ Department of Physics, University of Oslo, Oslo, Norway
- ¹²¹ Department of Physics, Oxford University, Oxford, United Kingdom
- ¹²² ^(a) INFN Sezione di Pavia; ^(b) Dipartimento di Fisica, Università di Pavia, Pavia, Italy
- ¹²³ Department of Physics, University of Pennsylvania, Philadelphia PA, United States
- ¹²⁴ National Research Centre “Kurchatov Institute” B.P.Konstantinov Petersburg Nuclear Physics Institute, St. Petersburg, Russia
- ¹²⁵ ^(a) INFN Sezione di Pisa; ^(b) Dipartimento di Fisica E. Fermi, Università di Pisa, Pisa, Italy
- ¹²⁶ Department of Physics and Astronomy, University of Pittsburgh, Pittsburgh PA, United States
- ¹²⁷ ^(a) Laboratório de Instrumentação e Física Experimental de Partículas – LIP, Lisboa; ^(b) Faculdade de Ciências, Universidade de Lisboa, Lisboa; ^(c) Department of Physics, University of Coimbra, Coimbra; ^(d) Centro de Física Nuclear da Universidade de Lisboa, Lisboa; ^(e) Departamento de Física, Universidade do Minho, Braga; ^(f) Departamento de Física Teórica y del Cosmos and CAFPE, Universidad de Granada, Granada (Spain); ^(g) Dep Física and CEFITEC of Faculdade de Ciências e Tecnologia, Universidade Nova de Lisboa, Caparica, Portugal
- ¹²⁸ Institute of Physics, Academy of Sciences of the Czech Republic, Praha, Czech Republic
- ¹²⁹ Czech Technical University in Prague, Praha, Czech Republic
- ¹³⁰ Faculty of Mathematics and Physics, Charles University in Prague, Praha, Czech Republic
- ¹³¹ State Research Center Institute for High Energy Physics (Protvino), NRC KI, Russia
- ¹³² Particle Physics Department, Rutherford Appleton Laboratory, Didcot, United Kingdom
- ¹³³ ^(a) INFN Sezione di Roma; ^(b) Dipartimento di Fisica, Sapienza Università di Roma, Roma, Italy
- ¹³⁴ ^(a) INFN Sezione di Roma Tor Vergata; ^(b) Dipartimento di Fisica, Università di Roma Tor Vergata, Roma, Italy
- ¹³⁵ ^(a) INFN Sezione di Roma Tre; ^(b) Dipartimento di Matematica e Fisica, Università Roma Tre, Roma, Italy
- ¹³⁶ ^(a) Faculté des Sciences Ain Chock, Réseau Universitaire de Physique des Hautes Energies – Université Hassan II, Casablanca; ^(b) Centre National de l’Energie des Sciences Techniques Nucleaires, Rabat; ^(c) Faculté des Sciences Semlalia, Université Cadi Ayyad, LPHEA-Marrakech; ^(d) Faculté des Sciences, Université Mohamed Premier and LPTPM, Oujda; ^(e) Faculté des sciences, Université Mohammed V, Rabat, Morocco
- ¹³⁷ DSM/IRFU (Institut de Recherches sur les Lois Fondamentales de l’Univers), CEA Saclay (Commissariat à l’Energie Atomique et aux Energies Alternatives), Gif-sur-Yvette, France
- ¹³⁸ Santa Cruz Institute for Particle Physics, University of California Santa Cruz, Santa Cruz CA, United States
- ¹³⁹ Department of Physics, University of Washington, Seattle WA, United States
- ¹⁴⁰ Department of Physics and Astronomy, University of Sheffield, Sheffield, United Kingdom
- ¹⁴¹ Department of Physics, Shinshu University, Nagano, Japan
- ¹⁴² Fachbereich Physik, Universität Siegen, Siegen, Germany

- ¹⁴³ Department of Physics, Simon Fraser University, Burnaby BC, Canada
¹⁴⁴ SLAC National Accelerator Laboratory, Stanford CA, United States
¹⁴⁵ ^(a) Faculty of Mathematics, Physics & Informatics, Comenius University, Bratislava; ^(b) Department of Subnuclear Physics, Institute of Experimental Physics of the Slovak Academy of Sciences, Kosice, Slovak Republic
¹⁴⁶ ^(a) Department of Physics, University of Cape Town, Cape Town; ^(b) Department of Physics, University of Johannesburg, Johannesburg; ^(c) School of Physics, University of the Witwatersrand, Johannesburg, South Africa
¹⁴⁷ ^(a) Department of Physics, Stockholm University; ^(b) The Oskar Klein Centre, Stockholm, Sweden
¹⁴⁸ Physics Department, Royal Institute of Technology, Stockholm, Sweden
¹⁴⁹ Departments of Physics & Astronomy and Chemistry, Stony Brook University, Stony Brook NY, United States
¹⁵⁰ Department of Physics and Astronomy, University of Sussex, Brighton, United Kingdom
¹⁵¹ School of Physics, University of Sydney, Sydney, Australia
¹⁵² Institute of Physics, Academia Sinica, Taipei, Taiwan
¹⁵³ Department of Physics, Technion: Israel Institute of Technology, Haifa, Israel
¹⁵⁴ Raymond and Beverly Sackler School of Physics and Astronomy, Tel Aviv University, Tel Aviv, Israel
¹⁵⁵ Department of Physics, Aristotle University of Thessaloniki, Thessaloniki, Greece
¹⁵⁶ International Center for Elementary Particle Physics and Department of Physics, The University of Tokyo, Tokyo, Japan
¹⁵⁷ Graduate School of Science and Technology, Tokyo Metropolitan University, Tokyo, Japan
¹⁵⁸ Department of Physics, Tokyo Institute of Technology, Tokyo, Japan
¹⁵⁹ Department of Physics, University of Toronto, Toronto ON, Canada
¹⁶⁰ ^(a) TRIUMF, Vancouver BC; ^(b) Department of Physics and Astronomy, York University, Toronto ON, Canada
¹⁶¹ Faculty of Pure and Applied Sciences, and Center for Integrated Research in Fundamental Science and Engineering, University of Tsukuba, Tsukuba, Japan
¹⁶² Department of Physics and Astronomy, Tufts University, Medford MA, United States
¹⁶³ Department of Physics and Astronomy, University of California Irvine, Irvine CA, United States
¹⁶⁴ ^(a) INFN Gruppo Collegato di Udine, Sezione di Trieste, Udine; ^(b) ICTP, Trieste; ^(c) Dipartimento di Chimica, Fisica e Ambiente, Università di Udine, Udine, Italy
¹⁶⁵ Department of Physics and Astronomy, University of Uppsala, Uppsala, Sweden
¹⁶⁶ Department of Physics, University of Illinois, Urbana IL, United States
¹⁶⁷ Instituto de Física Corpuscular (IFIC) and Departamento de Física Atomica, Molecular y Nuclear and Departamento de Ingeniería Electrónica and Instituto de Microelectrónica de Barcelona (IMB-CNM), University of Valencia and CSIC, Valencia, Spain
¹⁶⁸ Department of Physics, University of British Columbia, Vancouver BC, Canada
¹⁶⁹ Department of Physics and Astronomy, University of Victoria, Victoria BC, Canada
¹⁷⁰ Department of Physics, University of Warwick, Coventry, United Kingdom
¹⁷¹ Waseda University, Tokyo, Japan
¹⁷² Department of Particle Physics, The Weizmann Institute of Science, Rehovot, Israel
¹⁷³ Department of Physics, University of Wisconsin, Madison WI, United States
¹⁷⁴ Fakultät für Physik und Astronomie, Julius-Maximilians-Universität, Würzburg, Germany
¹⁷⁵ Fakultät für Mathematik und Naturwissenschaften, Fachgruppe Physik, Bergische Universität Wuppertal, Wuppertal, Germany
¹⁷⁶ Department of Physics, Yale University, New Haven CT, United States
¹⁷⁷ Yerevan Physics Institute, Yerevan, Armenia
¹⁷⁸ Centre de Calcul de l'Institut National de Physique Nucléaire et de Physique des Particules (IN2P3), Villeurbanne, France

^a Also at Department of Physics, King's College London, London, United Kingdom.

^b Also at Institute of Physics, Azerbaijan Academy of Sciences, Baku, Azerbaijan.

^c Also at Novosibirsk State University, Novosibirsk, Russia.

^d Also at TRIUMF, Vancouver BC, Canada.

^e Also at Department of Physics & Astronomy, University of Louisville, Louisville, KY, United States.

^f Also at Department of Physics, California State University, Fresno CA, United States.

^g Also at Department of Physics, University of Fribourg, Fribourg, Switzerland.

^h Also at Departament de Física de la Universitat Autònoma de Barcelona, Barcelona, Spain.

ⁱ Also at Departamento de Física e Astronomia, Faculdade de Ciências, Universidade do Porto, Portugal.

^j Also at Tomsk State University, Tomsk, Russia.

^k Also at Università di Napoli Parthenope, Napoli, Italy.

^l Also at Institute of Particle Physics (IPP), Canada.

^m Also at National Institute of Physics and Nuclear Engineering, Bucharest, Romania.

ⁿ Also at Department of Physics, St. Petersburg State Polytechnical University, St. Petersburg, Russia.

^o Also at Department of Physics, The University of Michigan, Ann Arbor MI, United States.

^p Also at Centre for High Performance Computing, CSIR Campus, Rosebank, Cape Town, South Africa.

^q Also at Louisiana Tech University, Ruston LA, United States.

^r Also at Institutio Catalana de Recerca i Estudis Avancats, ICREA, Barcelona, Spain.

^s Also at Graduate School of Science, Osaka University, Osaka, Japan.

^t Also at Department of Physics, National Tsing Hua University, Taiwan.

^u Also at Institute for Mathematics, Astrophysics and Particle Physics, Radboud University Nijmegen/Nikhef, Nijmegen, Netherlands.

^v Also at Department of Physics, The University of Texas at Austin, Austin TX, United States.

^w Also at Institute of Theoretical Physics, Iliia State University, Tbilisi, Georgia.

^x Also at CERN, Geneva, Switzerland.

^y Also at Georgian Technical University (GTU), Tbilisi, Georgia.

^z Also at Ochadai Academic Production, Ochanomizu University, Tokyo, Japan.

^{aa} Also at Manhattan College, New York NY, United States.

^{ab} Also at Hellenic Open University, Patras, Greece.

^{ac} Also at Academia Sinica Grid Computing, Institute of Physics, Academia Sinica, Taipei, Taiwan.

^{ad} Also at School of Physics, Shandong University, Shandong, China.

^{ae} Also at Moscow Institute of Physics and Technology State University, Dolgoprudny, Russia.

^{af} Also at Section de Physique, Université de Genève, Geneva, Switzerland.

^{ag} Also at Eotvos Lorand University, Budapest, Hungary.

^{ah} Also at International School for Advanced Studies (SISSA), Trieste, Italy.

^{ai} Also at Department of Physics and Astronomy, University of South Carolina, Columbia SC, United States.

^{aj} Also at School of Physics and Engineering, Sun Yat-sen University, Guangzhou, China.

^{ak} Also at Institute for Nuclear Research and Nuclear Energy (INRNE) of the Bulgarian Academy of Sciences, Sofia, Bulgaria.

^{al} Also at Faculty of Physics, M.V. Lomonosov Moscow State University, Moscow, Russia.

^{am} Also at Institute of Physics, Academia Sinica, Taipei, Taiwan.

^{an} Also at National Research Nuclear University MEPhI, Moscow, Russia.

^{ao} Also at Department of Physics, Stanford University, Stanford CA, United States.

^{ap} Also at Institute for Particle and Nuclear Physics, Wigner Research Centre for Physics, Budapest, Hungary.

^{aq} Also at Flensburg University of Applied Sciences, Flensburg, Germany.

^{ar} Also at University of Malaya, Department of Physics, Kuala Lumpur, Malaysia.

^{as} Also at CPPM, Aix-Marseille Université and CNRS/IN2P3, Marseille, France.

^{at} Also affiliated with PKU-CHEP.

* Deceased.